Supporting Information

Intramolecularly stapled amphiphatic peptides via boron-sugar interaction

Monika Kijewska*[a], Angelika Czerwińska[a], Samah Al Harthi[b], Grzegorz Wołczański[a], Mateusz Waliczek[a], Abdul-Hamid Emwas[b], Mariusz Jaremko[b], Łukasz Jaremko[b], Piotr Stefanowicz[a] and Zbigniew Szewczuk[a]

[a]*Faculty of Chemistry, University of Wrocław, Joliot-Curie 14, 50-383 Wrocław, Poland*

[b] *King Abdullah University of Science and Technology (KAUST), Biological and Environmental Sciences & Engineering Division (BESE), Thuwal, 23955-6900, Saudi Arabia.*

Corresponding author: Monika Kijewska,

Faculty of Chemistry, University of Wrocław,

F. Joliot-Curie 14, 50-383 Wrocław, Poland,

Fax: +48-71-3282348, Tel.: +48-71-3757250,

E-mail: monika.kijewska@chem.uni.wroc.pl

Table content

1. General information

Purification of staple peptides (HPLC analysis): The crude products were characterized by HPLC on a C18 column. Solvent systems: S1: 0.1% aqueous TFA, S2: 80% acetonitrile + 0.1% TFA, linear gradient from 0-80% of S2 for 40 min, flow rate 1.0 mL/min, UV detection at 210 nm. The main reaction products were purified by a preparative reversed-phase HPLC on a Vydac C18 column (22 mm × 250 mm), using solvent systems: S1: 0.1% aqueous TFA, S2: 40% acetonitrile + 0.1% TFA, linear gradient was individually set for each compound, flow rate 7.0 mL/min, UV detection at 210 nm. The fractions were collected and lyophilized. Their identities were confirmed on the basis of molecular weights measured with a Apex-Qe 7T instrument equipped with an electrospray ionization source.

ESI-MS experiments: High resolution mass spectra were measured using an Apex-Qe 7T instrument (Bruker) equipped with a dual ESI source. The acetonitrile/water/formic acid (50:50:0.1) mixture or methanol were used as solvents for recording the mass spectra. The potential between the spray needle and the orifice was set to 4.5 kV. In the MS/MS mode, the quadrupole was used to select the precursor ions, which were fragmented in the hexapole collision cell applying argon as a target gas. The obtained fragments were subsequently mass analysed by the ICR mass analyzer. For the collision-induced dissociation (CID) MS/MS measurements, the voltage over the hexapole collision cell varied from 15 to 30 V and argon was used as a collision gas.

LC-MS analysis: The LC-MS analysis was performed on Shimadzu LC IT-TOF. Separation was carried out on an RP-Zorbax (50×2.1 mm, 3.5 µm) column with a gradient elution of 0-50% B in A (A = 0.1% HCOOH in water; B = 0.1% HCOOH in MeCN) at room temperature over a period of 20 min (flow rate: 0.1 mL/min).

Enzymatic hydrolysis: Enzymatic hydrolysis was performed according the protocol published by Stefanowicz *et al.*[1]. Briefly, 1 mg of peptide was dissolved in 200 µl of 50 mM ammonium bicarbonate buffer. Then trypsin stock solution (1 mg in 1000 µl in water) was added to reach the enzyme:substrate mass ratio of 1:20 and incubated for 12 h at 37°C. Digestion was terminated by the addition of 10 µl of formic acid. The resulting digest was lyophilized and used for MS experiments.

NMR spectroscopy: All NMR measurements for model peptides and modified MAP analougs were carried out at 25 °C, at the peptide concentration of 1-2 mg mL^{-1}, in 99% D_2O, using Bruker 950 MHz AVANAC III NMR spectrometer equipped with Bruker TCI cro-probe (BrukerBioSpin, Rheinstetten, Germany). The complete proton resonance assignment of the Fru1PhB2 and Fru1PhB3 peptide spin systems were accomplished on the basis of 2D ^{1}H–^{1}H TOCSY (80 ms mixing times) and ^{1}H–^{1}H NOESY (100 and 300 ms) spectra. All ^{11}B NMR spectra were recorded using Bruker 600 MHz AVANAC III NMR spectrometer equipped with Bruker BBOF probe (BrukerBioSpin, Rheinstetten, Germany). For comparative analysis, all NMR

[1] P. Stefanowicz, M. Kijewska, A. Kluczyk, Z. Szewczuk, *Anal. Biochem*., 2010, **400**, 237.

experiments were carried out under the same instrumental parameters and experimental conditions. To element the ^{11}B background form probe glass, each ^{11}B NMR spectrum was induced using spin echo with gradients sequence through a standard (zggpse) program from the Bruker pulse sequence library. All spectra were recorded at room temperature by collecting 5k sans with 2 sec recycle delay, and the delay for homospoil gradient recovery was optimized to 300 us. Bruker Topspin 3.5pl7 software (Bruker BioSpin, Rheinstetten, Germany) was used to collect the data and also used for data post-processing analysis.

Circular Dichroism (CD) Spectroscopy and Thermal Unfolding: The measurements were carried out using J-1500 Circular Dichroism Spectrophotometer equipped with a thermoelectrically controlled cell holder under a constant nitrogen flow. The peptides secondary structure was measured with far-UV (190-260 nm) and 0.1-mm of cuvette path length. Peptides concentration were 156uM Ac-MAP, 896uM Fru1PhB2, 358 uM Fru1PhB3, 645 uM Fru1PhB4, 1.18 mM Fru1PhB5, 0.05 mM Ac-RNase*, 0.035 mM Fru1PhB3*. For each CD spectrum an average of 10 scans of the same sample was collected at 25 °C with a step resolution of 0.1 nm, a scan speed of 50 nm per minute and a bandwidth of 1 nm. The data were processed by Spectra Manager Analysis software provided from JASCO as follows: the spectrum of each sample was corrected to baseline, smoothed with Savitsky-Golay filter and converted to molar ellipticity. Following CD measurements, the percentages of secondary structure content of the peptides are estimated by using JASCO's CD multivariate Secondary Structure Estimation (SSE) analysis program. This program estimates the secondary structure (helix, sheet and random coil) contents of unknown sample from CD spectrum obtained by using the multivariate analysis technique[2]. It includes the CD spectra (176 - 260 nm) of 26 types of proteins measured by JASCO and the calibration models created based on these data. In this program, two precise multivariate analysis methods are adopted, Partial Least Squares (PLS) and Principal Component Regression (PCR) methods. In both methods, the spectra are compressed to a few potential factors, and the concentration is indicated based on such potential factors. Then abundance ratio of secondary structure is calculated so that the residual error of the concentration may be the minimum.**[2]** To investigate the peptide thermal stability, the thermal unfolding curve was measured by recording far-UV CD spectra as a function of temperature between 20 and 90°C in steps of 0.2 °C with an equilibration time of 1 min at each temperature. The denaturation temperature was attained by monitoring 222 and 208 nm wavelengths and Tm obtained with ±1 °C deviation.

2. Experimental section

The derivatives of amino acids for peptide synthesis and the coupling reagent (TBTU - O-(Benzotriazol-1-yl)-*N,N,N',N'*-tetramethyluronium tetrafluoroborate, PyBop - (benzotriazol-1-yl-oxytripyrrolidinophosphonium hexafluorophosphate) were purchased from NovaBiochem. The ChemMatrix Rink Resin (0.4-0.60 mmol/g), 4-carboxyphenylboronic acid were purchased from Sigma-Aldrich. The solvents for peptide synthesis (analytical grade) were obtained from Riedel de Haën (DMF) and J. T. Baker (methanol, acetonitryle). Fmoc-Lys(*i,i*-Fru,Boc)-OH was synthesized according the procedure published by Stefanowicz *et al*.[3] Other solvents used in

[2] **Application Note Booklet for CD spectrometer, JASCO Corporation, Japan, 2014**

this work were obtained from Aldrich. Other reagents used in this work were obtained from Aldrich: triisopropylsilane (TIS) and IrisBiotech: trifluoroacetic acid, N,N-diisopropylethylamine (DIEA).

2.1 Experimental procedure

Synthesis of staple peptides (containing fructosylolysine moiety and phenylboronic acid): The staple peptides were synthesized according the standard Fmoc procedure with TBTU (3 eq.) as a coupling reagent using ChemMatrix® Rink Resin (loaded 0.4-0.6 mmol/g). The deoxyfructosylated lysine moiety (Fmoc-Lys(*i,i*-Fru,Boc)-OH) was synthesized according to Stefanowicz et al.[2] After synthesis the whole peptide sequence the peptide attached to resin was acetylated using Ac_2O:DIEA:DMF (9:17:74, v:v:v), then the Mtt group was removed from ε-amino group of lysine moiety using 1% TFA in DCM and the coupling of 4-carboxyphenylboronic acid was carried out using PyBOP (3 eq.) and DIEA (6 eq.) in DMF for 4 h. After the reaction was completed the resin was washed: DMF (7×1 min), DCM (3×1 min), THF (3×1 min), MeOH (3×1 min) and Et_2O (3×1 min). The last step consisted of drying of a peptydylresin in vacuum desiccator for one day at room temperature The products were removed from resin using water/triisopropylsilan/trifluoracetic acid (2.5:2.5:95) for 8 h. After evaporating trifluoracetic acid the products were lyophilized and analyzed by analytical methods: ESI-MS, ESI-MS/MS, LC-MS, NMR and CD.

2.2 Analytical data

Table S1 The list of obtained peptides

Sequence	Abbreviation
Ac-KLALKLALKALKAALKLA-NH_2	**Ac-MAP**
Ac-cyclo(K(*i*-Fru)LALK(PhB))LALKALKAALKLA-NH_2	**Fru1PhB2**
Ac-cyclo(K(*i*-Fru)LALKLALK(PhB))ALKAALKLA-NH_2	**Fru1PhB3**
Ac-cyclo(K(*i*-Fru)LALKLALKALK(PhB))AALKLA-NH_2	**Fru1PhB4**
Ac-cyclo(K(*i*-Fru)LALKLALKALKAALK(PhB))LA-NH_2	**Fru1PhB5**
Ac-EWAEKAAAKFLKAHA-NH_2	**Ac-RNaseA***
Ac-EWAEcyclo(K(*i*-Fru)AAAKFLK(PhB))AHA-NH_2	**Fru1PhB3***

[3] P. Stefanowicz, M. Kijewska, K. Kapczyńska, Z. Szewczuk, *Amino Acids,* 2010, **38**, 881.

* C-terminal 15-peptide of RNaseA

2.2.1 Ac-KLALKLALKALKAALKLA-NH_2 (Ac-MAP)

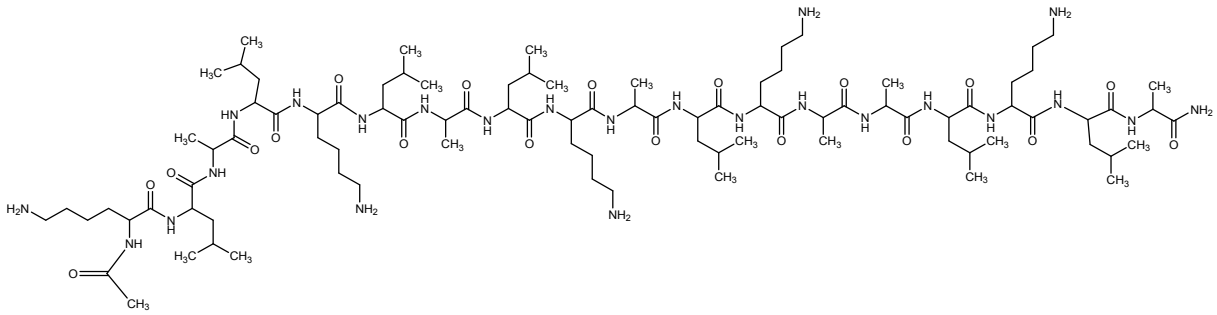

Yield: 80%

LC-IT-TOF (Rt): 16 min

ESI-FT-MS: $[M+2H]^{2+}$: 959.647 $[M+3H]^{3+}$:640.112

calc. *m/z* for $C_{92}H_{172}N_{24}O_{19}$: $[M+2H]^{2+}$:959.669 $[M+3H]^{3+}$:640.115

ESI-FT-MS/MS: precursor ion at *m/z* 960.157 ($[M+2H]^{2+}$); collision energy 12 eV: *m/z:* 915.633 (wartość obliczona dla $b17^{2+}$: 915.634); 859.091 (wartość obliczona dla $b16^{2+}$: 859.095); 1589.074 (calc. for b15: 1589.088); 1476.001 (calc. for b14: 1476.004); 1404.964 (calc. for b13: 1404.967); 1333.931 (calc. for b12: 1333.930); 1305.895 (calc. for a12: 1305.935); 1205.832 (calc. for b11: 1205.835); 1092.751 (calc. for b10: 1092.751); 1021.714 (calc. for b9: 1021.714); 893.617 (calc. for b8: 893.619); 780.534 (calc. for b7: 780.535); 696.474 (calc. for z7: 696.477); 596.413 (calc. for b5: 596.414); 568.382 (calc. for z6: 568.382).

2.2.2 Ac-cyclo(K(*i*-Fru)LALK(PhB))LALKALKAALKLA-NH_2 (Fru1PhB2)

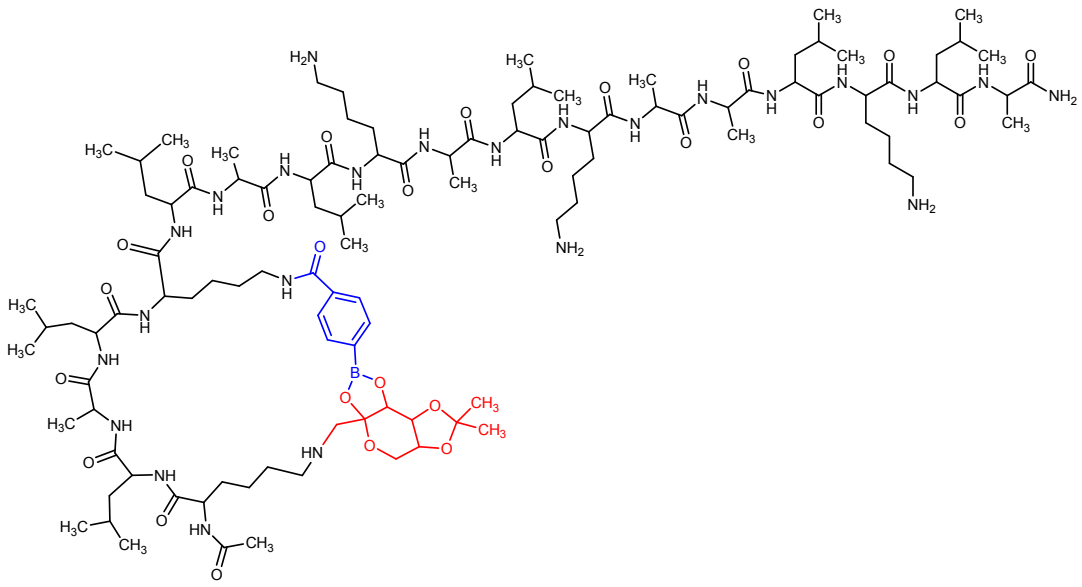

Yield: 70%

LC-IT-TOF (Rt): 17.5 min

ESI-FT-MS: m/z $[M+2H]^{2+}$: 1116.720; $[M+3H]^{3+}$: 744.815;

Calc. *m/z* for $C_{108}H_{187}BN_{24}O_{25}$: $[M+2H]^{2+}$: 1116.717; $[M+3H]^{3+}$:744.814;

ESI-FT-MS/MS: precursor ion at *m/z* 744.815 ($[M+3H]^{3+}$); collision energy 15 eV: *m/z*: 952.100 (calc. for $b15^{2+}$: 952.095); 760.474 (calc. for $b11^{2+}$: 760.469); 703.929 (calc. for $b10^{2+}$: 703.927); 1207.719 (calc. for b8: 1207.715); 1094.633 (calc. for b7: 1094.633); 1023.595 (calc. for b6: 1023.594); 910.511 (calc. for b5: 910.510); 880.598 (calc. for z9: 880.600); 809.654 (calc. for z8: 809.561); 568.382 (calc. for z6: 568.382); 497.345 (calc. for z5: 497.345); 897.628 (calc. for y9: 897.624); 826.591 (calc. for y8: 826.587).

2.2.3 Ac-cyclo(K(*i*-Fru)LALKLALK(PhB))ALKAALKLA-NH_2 (Fru1PhB3)

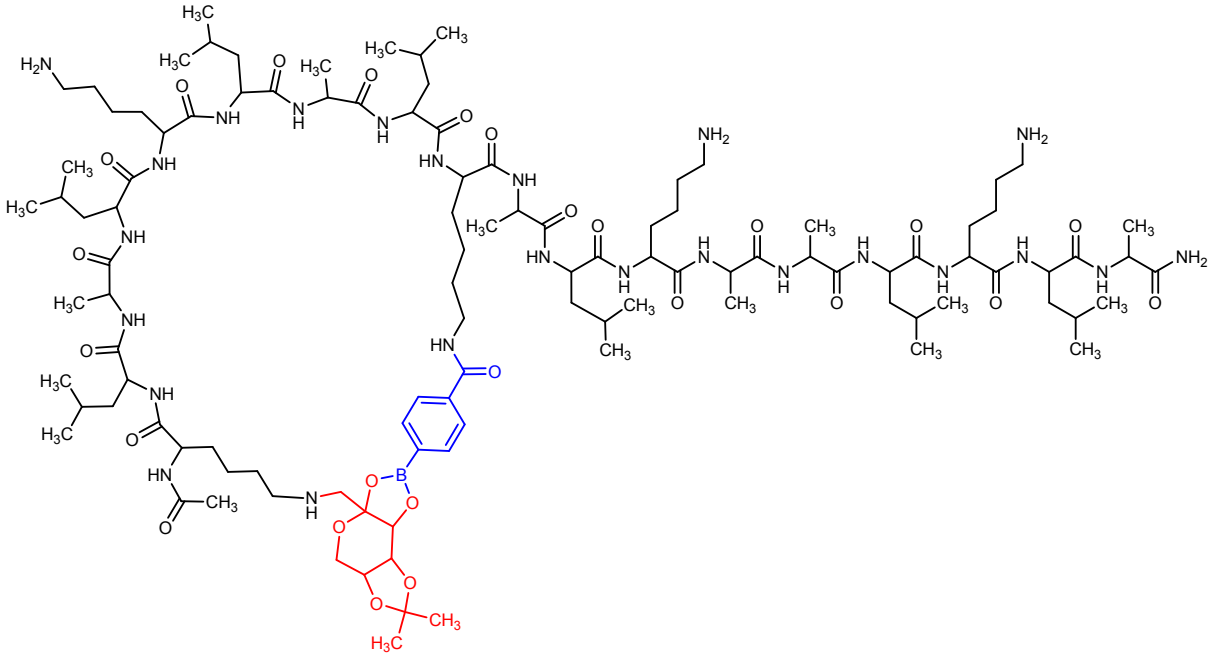

Yield: 75%

LC-IT-TOF (Rt): 17.4 min

ESI-FT-MS: m/z $[M+2H]^{2+}$: 1116.721; $[M+3H]^{3+}$: 744.818;

Calc. m/z for $C_{108}H_{187}BN_{24}O_{25}$: $[M+2H]^{2+}$: 1116.717; $[M+3H]^{3+}$:744.814;

ESI-FT-MS/MS: precursor ion at *m/z* 744.818 ([M+3H]3+); collision energy 15 eV or 18 eV: *m/z*: 952.105 (calc. for $b15^{2+}$: 952.095); 895.562 (calc. for $b14^{2+}$: 895.553); 860.043 (calc. for $b13^{2+}$: 860.035); 824.524 (calc. for $b12^{2+}$: 824.517); 1519.955 (calc. for b11: 1519.931); 1406.855 (calc. for b10: 1406.847); 1335.819 (calc. for b9: 1335.810); 809.567 (calc. for z8: 809.561); 568,385 (calc. for z6: 568.382); 497.347 (calc. for z5: 497.345).

2.2.4 Ac-cyclo(K(*i*-Fru)LALKLALKALK(PhB))AALKLA-NH_2 (Fru1PhB4)

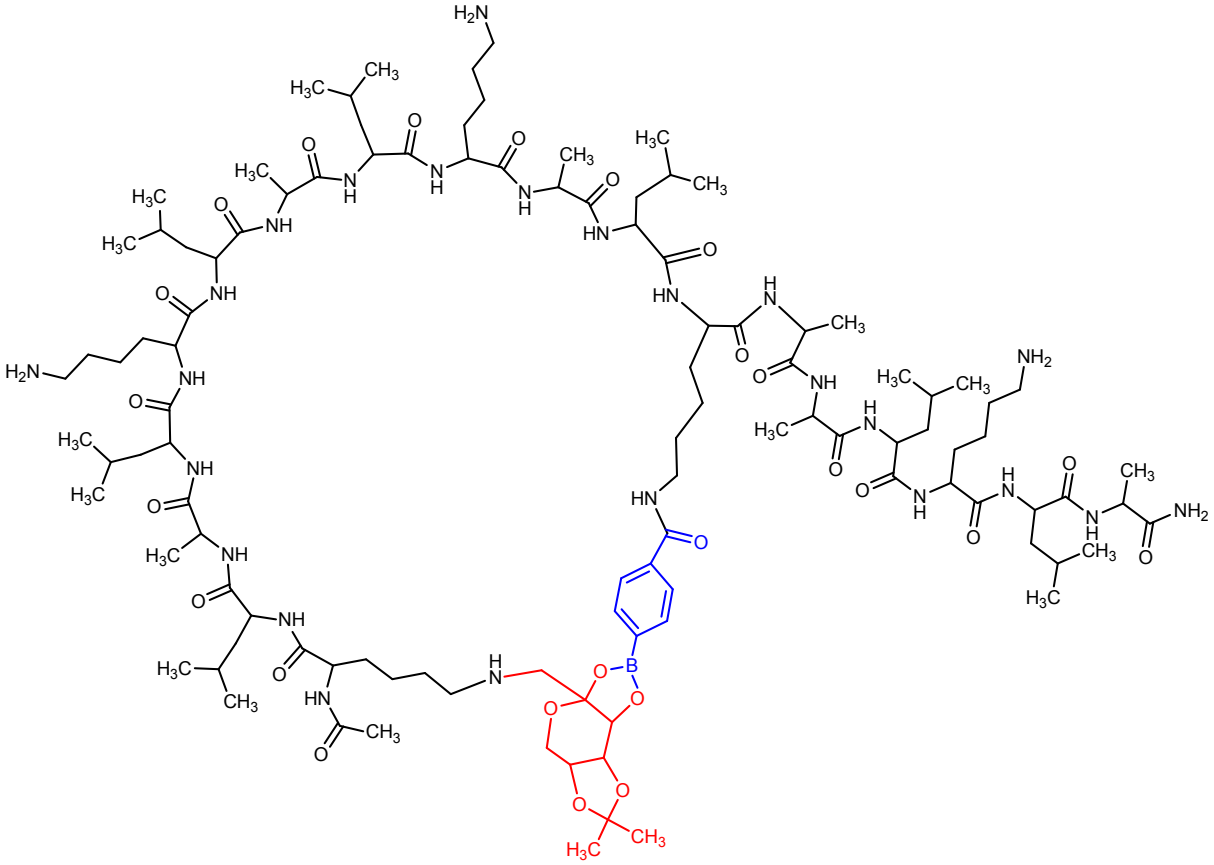

Yield: 68%

LC-IT-TOF (Rt): 17.4 min

ESI-FT-MS: *m/z* $[M+2H]^{2+}$: 1116.727; $[M+3H]^{3+}$: 744.820;

Calc. *m/z* for $C_{108}H_{187}BN_{24}O_{25}$: $[M+2H]^{2+}$: 1116.717; $[M+3H]^{3+}$:744.814;

ESI-FT-MS/MS: precursor ion at *m/z* 744.820 ($[M+3H]^{3+}$); collision energy 15 eV: *m/z*: 1072.687 (calc. for $b17^{2+}$: 1072.685); 1016.147 (calc. for $b16^{2+}$: 1016.143); 952.098 (calc. for $b15^{2+}$: 952.096); 895.555 (calc. for $b14^{2+}$: 896.554); 860.036 (calc. for $b13^{2+}$: 860.035); 824.519 (calc. for $b12^{2+}$: 824.516); 585.410 (calc. for y6: 585.408); 514.372 (calc. for y5: 514.371); 443.318 (calc. for y4: 443.304); 497.345 (calc. for z5: 497.345).

2.2.5 Ac-cyclo(K(*i*-Fru)LALKLALKALKAALK(PhB))LA-NH_2 (Fru1PhB5)

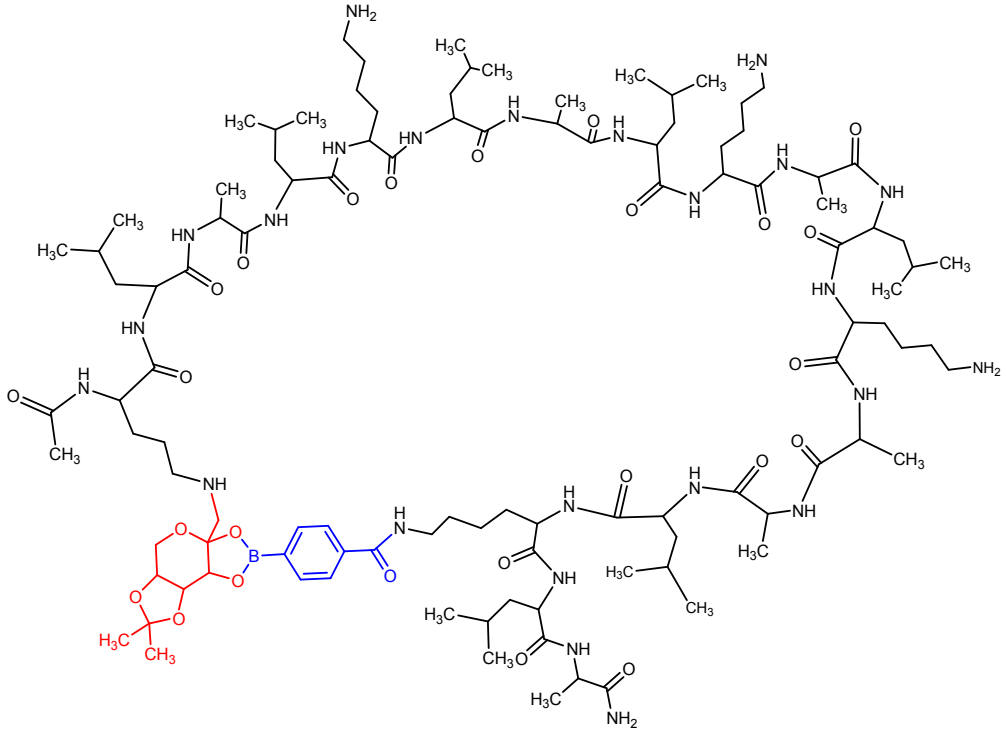

Yield: 74%

LC-IT-TOF (Rt): 17 min

ESI-FT-MS: *m/z* $[M+2H]^{2+}$: 1116.709; $[M+3H]^{3+}$: 744.806;

Calc. *m/z* for $C_{108}H_{187}BN_{24}O_{25}$: $[M+2H]^{2+}$: 1116.717; $[M+3H]^{3+}$:744.814;

ESI-FT-MS/MS: precursor ion at *m/z* 744.806 ($[M+3H]^{3+}$); collision energy 15 eV: *m/z*: 1072.696 (calc. for $b17^{2+}$: 1072.685); 1016.151 (calc. for $b16^{2+}$: 1016.143); 715.464 (calc. for $b17^{3+}$: 715.459).

2.2.6 PhB-Gly-Lys(*i*-Fru)-NH_2

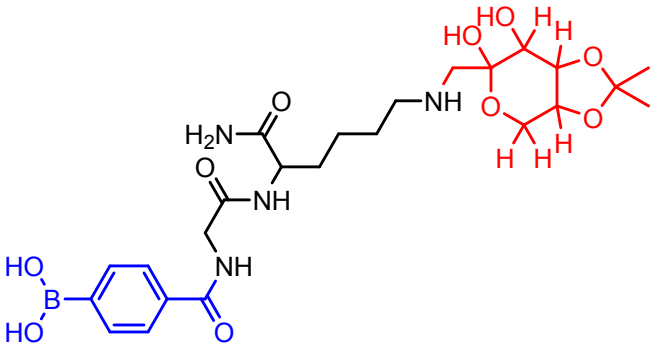

Yield: 85 %

LC-IT-TOF (Rt): 10 min

ESI-FT-MS: *m/z* $[M+H]^+$: 553.269

Calc. *m/z* for $C_{24}H_{36}BN_4O_{10}$: $[M+H]^+$: 553.267

^{1}H NMR (500 MHz, 300K, $CDCl_3$) δ = 1.36 - 1.44 (m, 2H), 1.35 (s, 3H), 1.47 (s, 3H), 1.6 - 1.76 (m, 2H), 1.8 - 1.88 (m, 2H), 2.99 - 3.08 (m, 2H), 3.23 (d, *J* = 13.4 Hz, 1H), 3.55 (d, *J* = 13.2 Hz, 1H), 3.64-3.68 (m, 1H), 3.77 (dd, J^{12} = 11.7 Hz, J^{13} = 4.9 Hz, 1H), 4.05 - 4.1 (m, 1H), 4.08 (d, J = 12.5 Hz , 2H), 4.12 - 4.14 (m, 1H), 4.2 (t, *J* = 3.6 Hz, 1H), 4.3 (dd, J^{12} = 9.61 Hz, J^{13} = 5 Hz, 1H), 7.72 - 7.82 (m, 4H); **^{13}C NMR** (150 MHz, 300K, $CDCl_3$) δ = 25, 27.4, 28.1, 29.2, 33.3, 46, 51.1, 52.7, 56.1, 65.5, 66.1, 68.7, 81.4, 102.5, 115.5, 117.9, 129.4, 136.7, 137.5, 139.8, 174.1, 174.5, 179.5

2.2.7 PhB-βAla-βAla-βAla-Lys(*i*-Fru)-NH_2

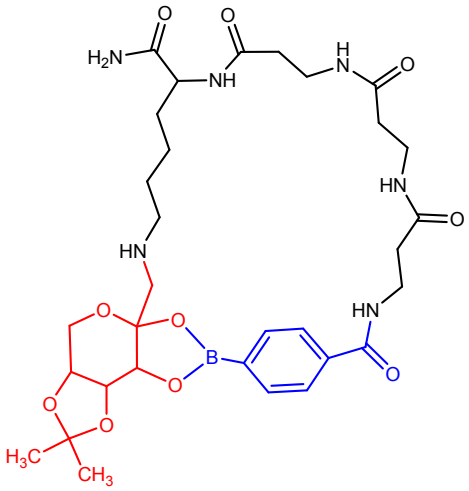

Cyclic form ESI-FT-MS: *m/z* $[M+H]^+$: 673.341
Calc. *m/z* for $C_{31}H_{45}BN_6O_{10}$: $[M+H]^+$: 673.337

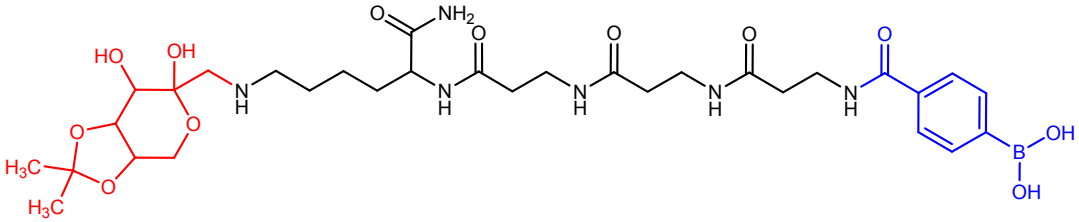

Linear form: ESI-FT-MS: *m/z* $[M+H]^+$: 709.353
Calc. *m/z* for $C_{31}H_{49}BN_6O_{12}$: $[M+H]^+$: 709.358

2.2.8 PhB-βAla-βAla-βAla-Lys(*i*-Fru)-NH_2

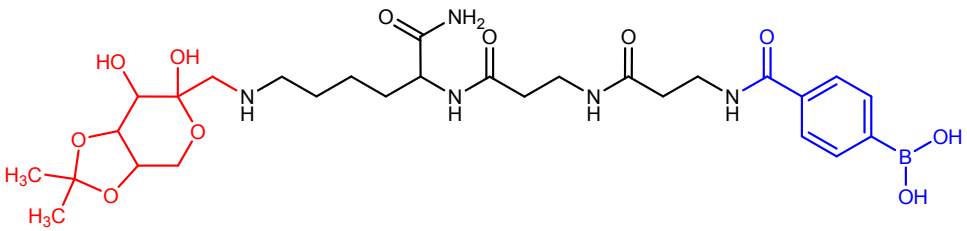

Linear form: ESI-FT-MS: *m/z* $[M+H]^+$: 638.320
Calc. *m/z* for $C_{28}H_{44}BN_5O_{11}$: $[M+H]^+$: 638.320

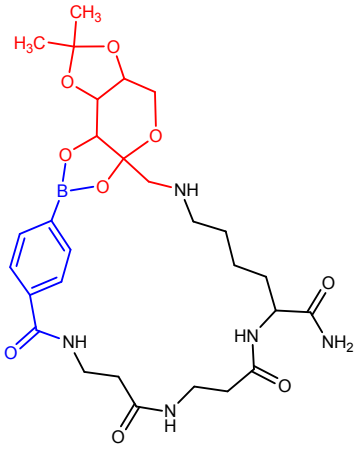

Cyclic form: ESI-FT-MS: *m/z* $[M+H]^+$: 602.303
Calc. *m/z* for $C_{28}H_{40}BN_5O_9$: $[M+H]^+$: 602.299

2.2.9 Ac-RNaseA* (Ac-EWAEKAAAKFLKAHA-NH_2)

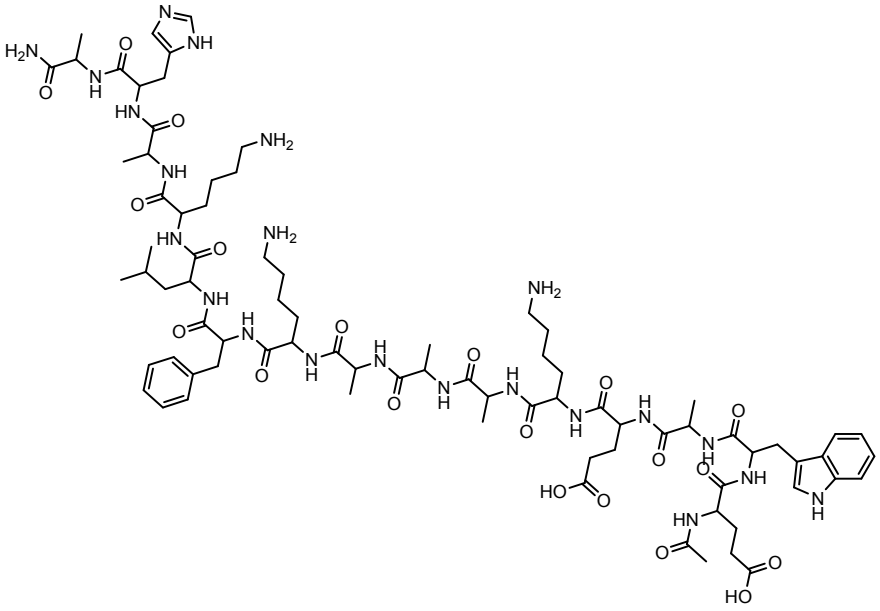

Yield: 75%

LC-IT-TOF (Rt): 6 min

ESI-FT-MS: *m/z* $[M+3H]^{3+}$: 571.315; $[M+2H]^{2+}$: 856,450

Calc. *m/z* for $C_{80}H_{122}N_{22}O_{20}$: $[M+3H]^{3+}$:571.314; $[M+2H]^{2+}$: 856,451

ESI-FT-MS/MS: precursor ion at *m/z* 856.450 ($[M+3H]^{3+}$); collision energy 22 eV: *m/z*: 1486.752 (calc for b_{13}: 1486.805); 1415,721 (calc. for b_{12}: 1415.768); 1287.633 (calc. for b_{11}: 1287.673);

1174.557 (calc. for b_{10}: 1174.589); 1137.659 (calc. for z_{11}: 1137.689); 1027.496 (calc. for b_9: 1027.520); 1026.596 (calc. for y_{10}: 1026.620); 1009.570 (calc. for z_{10}: 1009.594); 955.562 (calc. for y_9: 955.583); 938.537 (calc. for z_9: 938.557); 867.503 (calc. for z_8: 867.520); 796.486 (calc. for z_7: 796.483); 757.338 (calc. for b_6: 757.351); 685.403 (calc. for y_6: 685.414); 668,378 (calc. for z_6: 668.388); 558.212 (calc. for b_4: 558.219); 521.313 (calc. for z_5: 521.319); 429,172 (calc. for b_3: 429.177); 408.231 (calc. for z_4: 408.235); 358.136 (calc. for b_2: 358.139)

2.2.10 Fru1PhB3* (Ac-EWAEcyclo(K(i-Fru)AAAKFLK(PhB))AHA-NH_2)

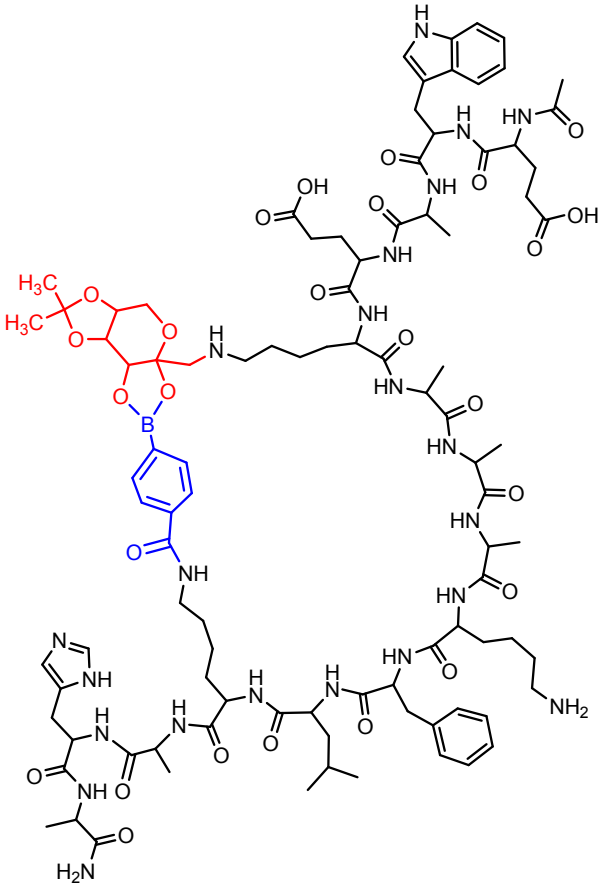

(*modified analogue of C peptide sequence of RNaseA)

Yield: 71%

LC-IT-TOF (Rt): 7 min

ESI-FT-MS: *m/z* $[M+2H]^{2+}$: 1013.493; $[M+3H]^{3+}$: 676.005;

Calc. *m/z* for $C_{96}H_{137}BN_{22}O_{26}$: $[M+2H]^{2+}$: 1013.515; $[M+3H]^{3+}$:676.013;

ESI-FT-MS/MS: precursor ion at *m/z* 1013.493 ($[M+3H]^{3+}$); collision energy 30 eV: *m/z*: 1800.825 (calc. for b_{13}: 1800.901); 1729.805 (calc. for b_{12}: 1729.864); 1380.716 (calc. for $b_{14}y_{11}$ 1380.727); 1243.659 (calc. for $b_{13}y_{11}$ 1243.679); 1172.629 (calc. for $b_{12}y_{11}$ 1172.642); 969.467 (calc. for b_{14}^{2+} 969.484); 726.388 (calc. for $[z_{11}]^{2+}$: 726.396); 558.215 (calc. for b_4: 558.219); 429.173 (calc. for b_3: 429.177); 358.137 (calc. for b_2: 358.139)

3. LC-MS analysis

3.1 Ac-MAP

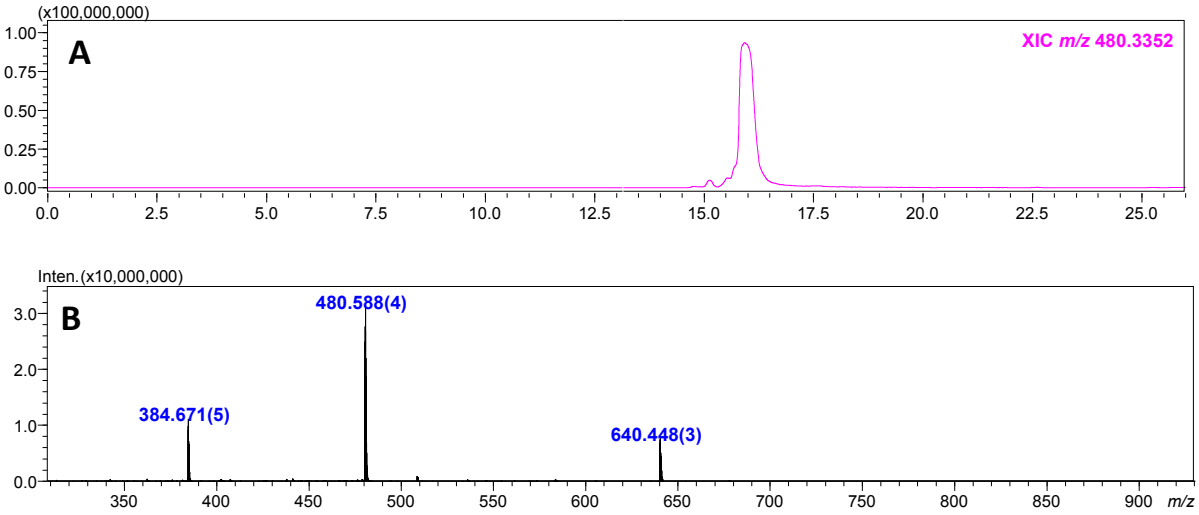

Fig. S1 LC-MS analysis of Ac-MAP a) XIC for *m/z* 480.335; b) ESI-MS spectrum.

3.2 Fru1PhB2

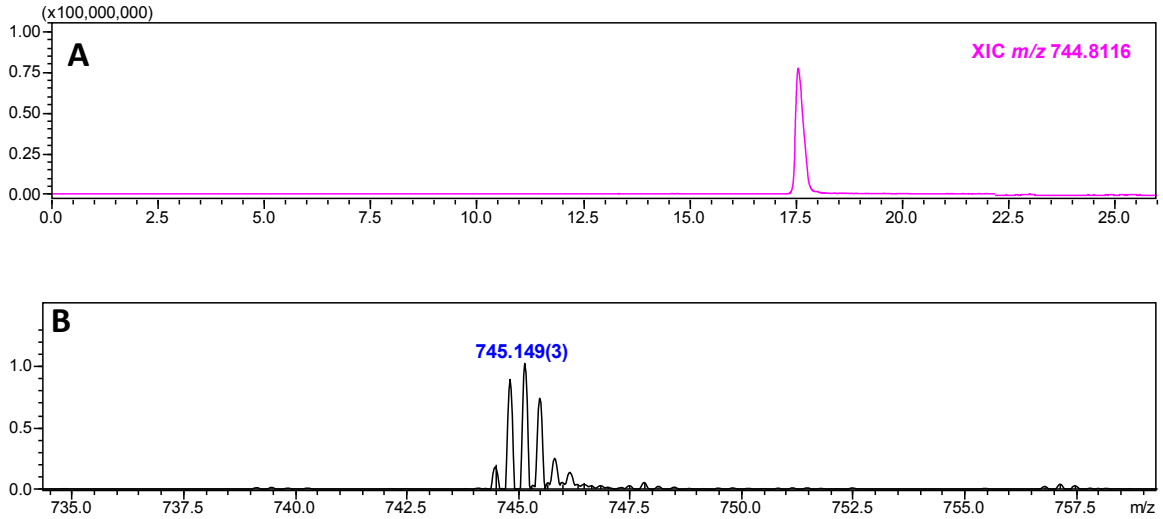

Fig. S2 LC-MS analysis of Fru1PhB2 a) XIC for *m/z* 745.149; b) ESI-MS spectrum (characteristic isotopic pattern).

3.3 Fru1PhB3

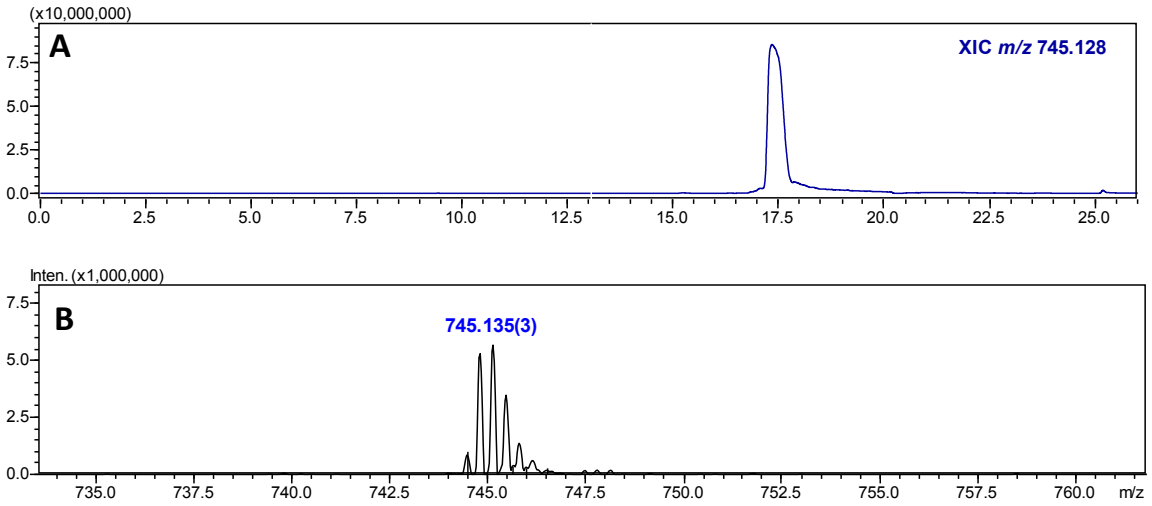

Fig. S3 LC-MS analysis of Fru1PhB3 a) XIC for *m/z* 745.128; b) ESI-MS spectrum (characteristic isotopic pattern).

3.4 Fru1PhB4

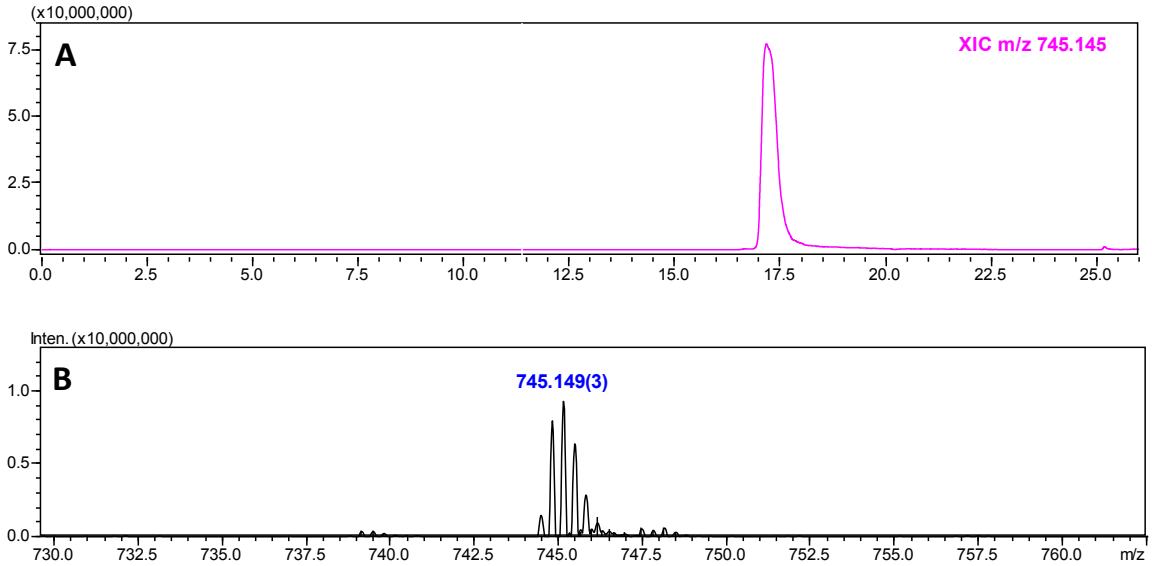

Fig. S4 LC-MS analysis of Fru1PhB4 a) XIC for *m/z* 745.145; b) ESI-MS spectrum (characteristic isotopic pattern).

3.5 Fru1PhB5

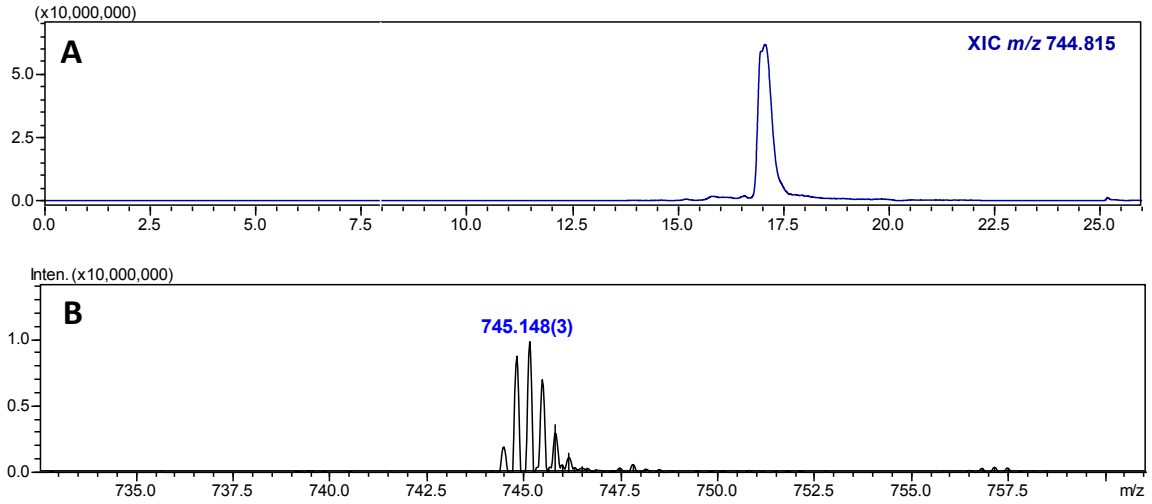

Fig. S5 LC-MS analysis of Fru1PhB5 a) XIC for *m/z* 745.148; b) ESI-MS spectrum (characteristic isotopic pattern).

3.6 Ac-RNaseA*

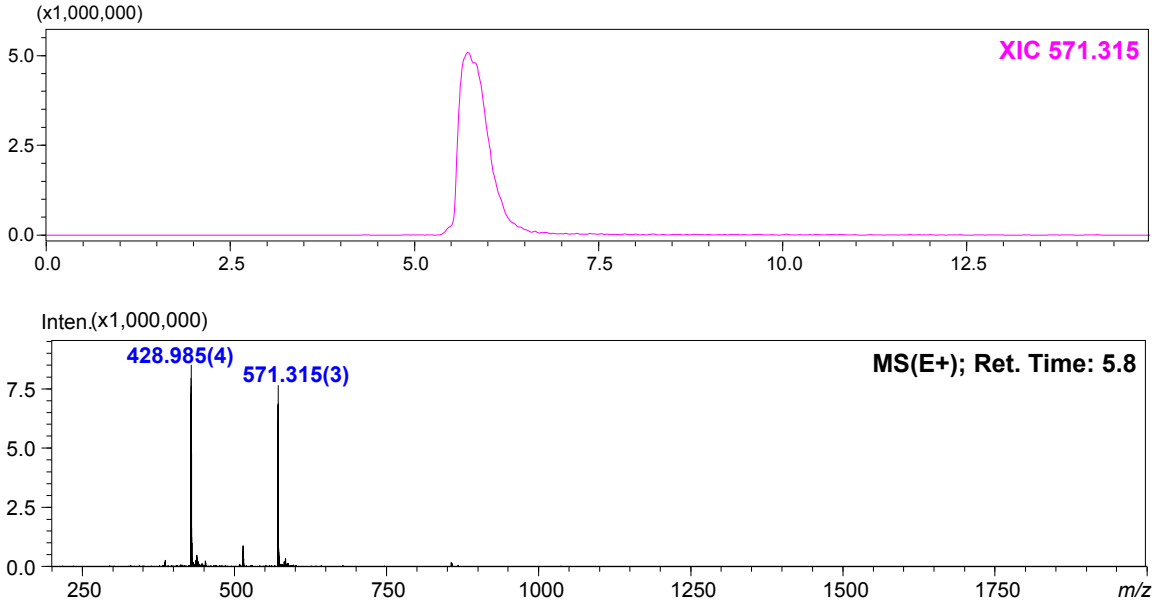

Fig. S6 LC-MS analysis of Ac-RNaseA* a) XIC for *m/z* 571.315; b) ESI-MS spectrum

3.7 Fru1PhB3*

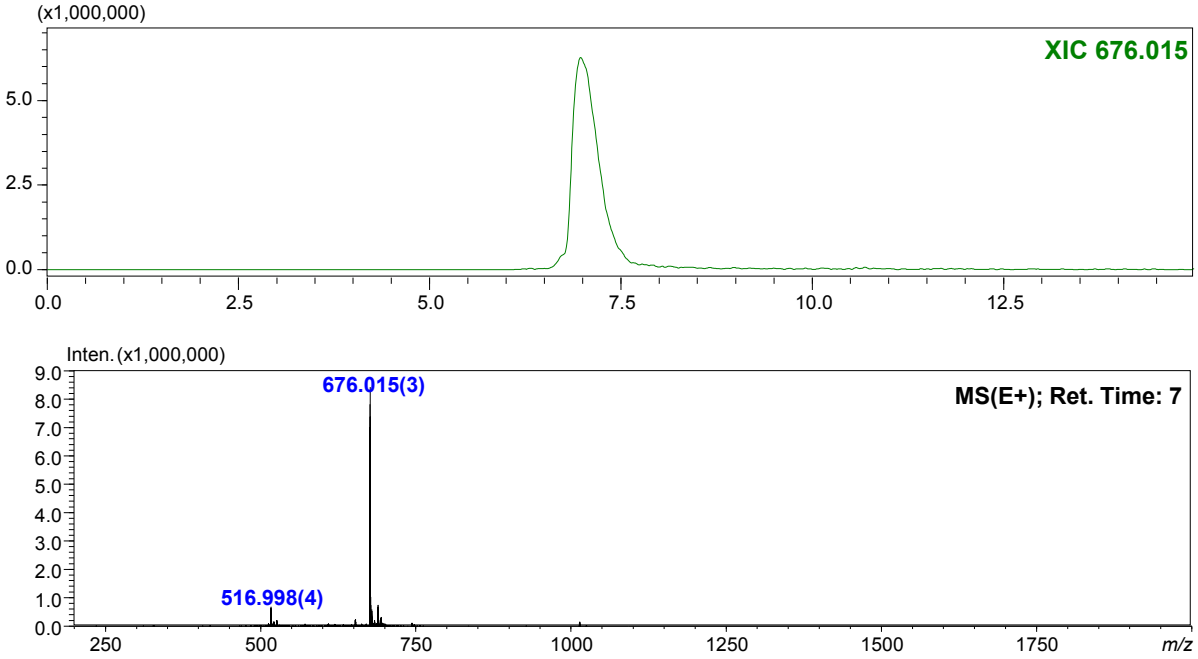

Fig. S7 LC-MS analysis of Fru1PhB3* (* - modified C peptide sequence of RNaseA) a) XIC for *m/z* 676.015; b) ESI-MS spectrum

4. ESI-MS and ESI-MS/MS spectra

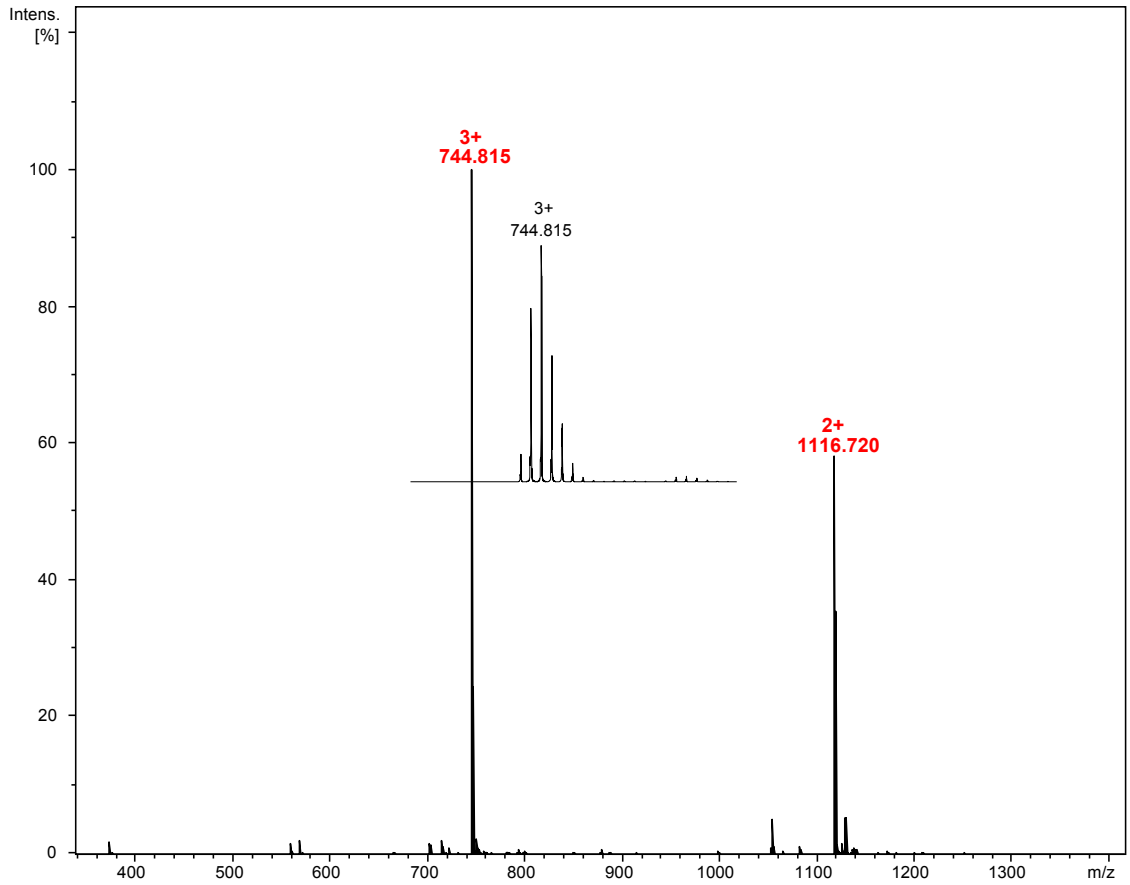

Fig. S8 ESI-MS spectrum of pure staple peptide Fru1PhB2

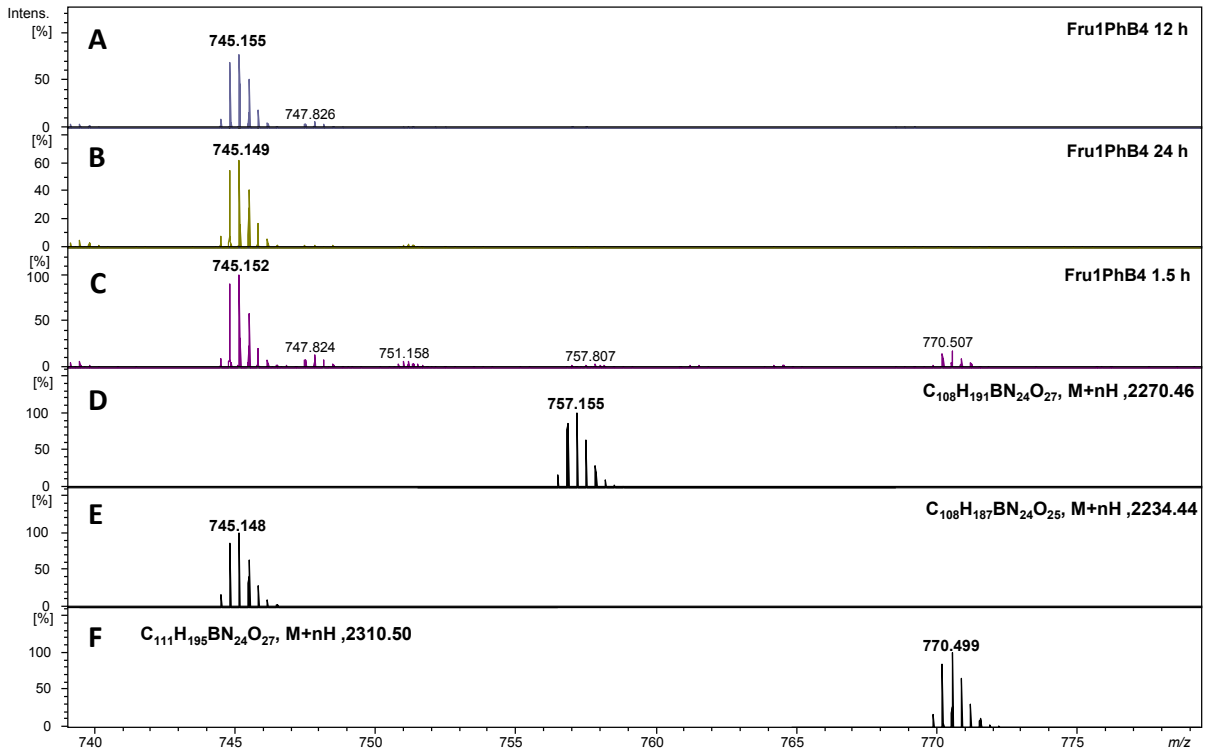

Fig. S9 ESI-MS spectra of peptide Fru1PhB4 (A-C - different time of peptide release from the resin; simulated spectra for obtained product (E) and for products with one and two protecting groups (D,F).

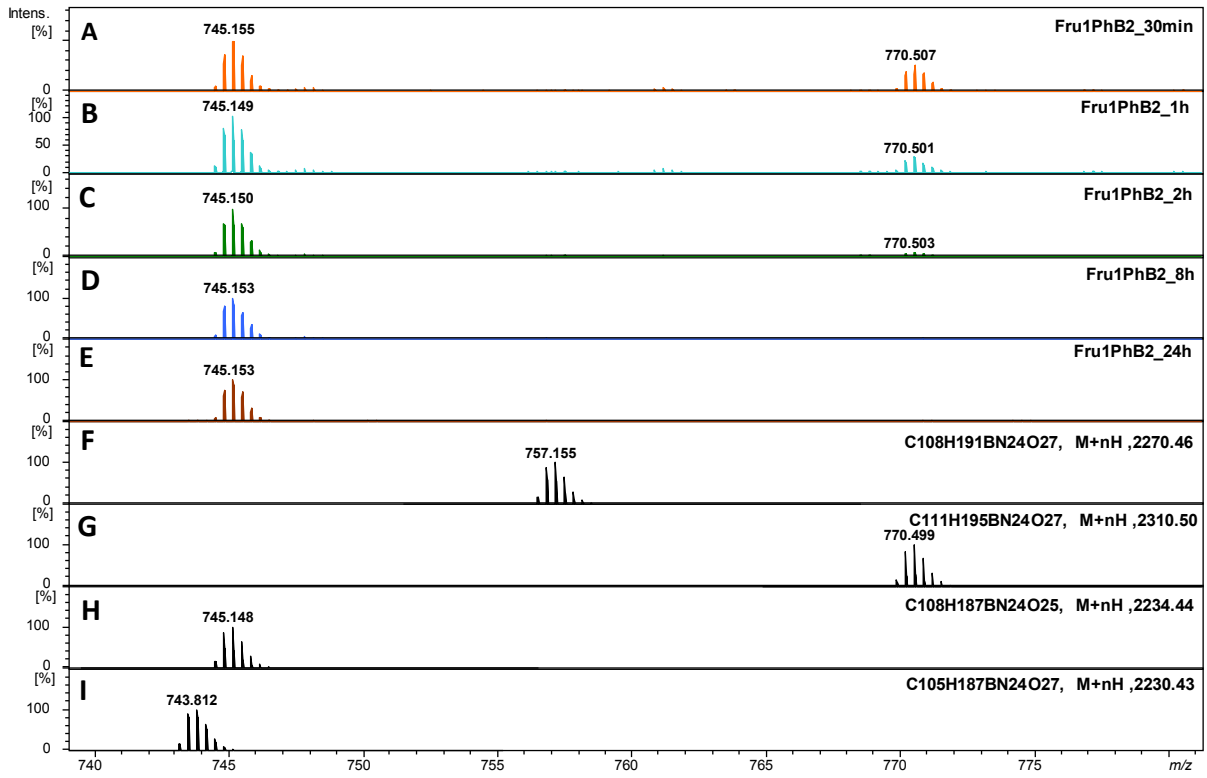

Fig. S10 ESI-MS spectra of peptide Fru1PhB2 (A-E - different time of peptide release from the resin; simulated spectra for obtained: staple product (H), linear products with one and two protecting groups (F, G) and linear product without protecting groups (I).

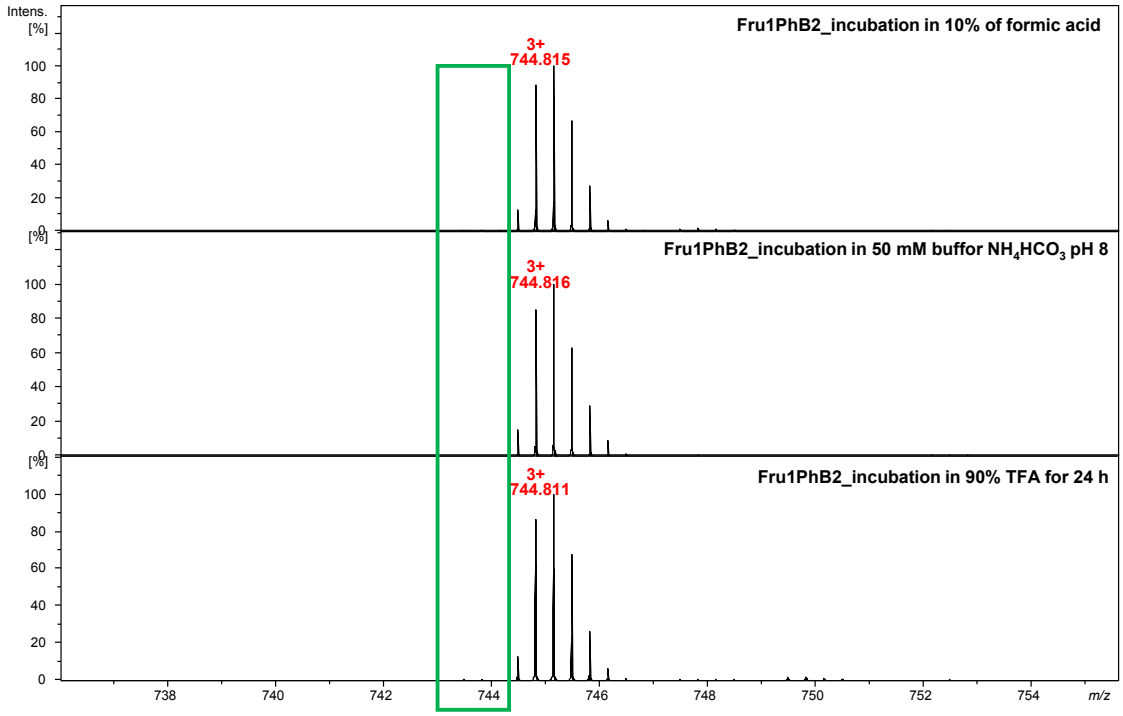

Fig. S11 ESI-MS spectra of peptide Fru1PhB2 (stability in different solution).

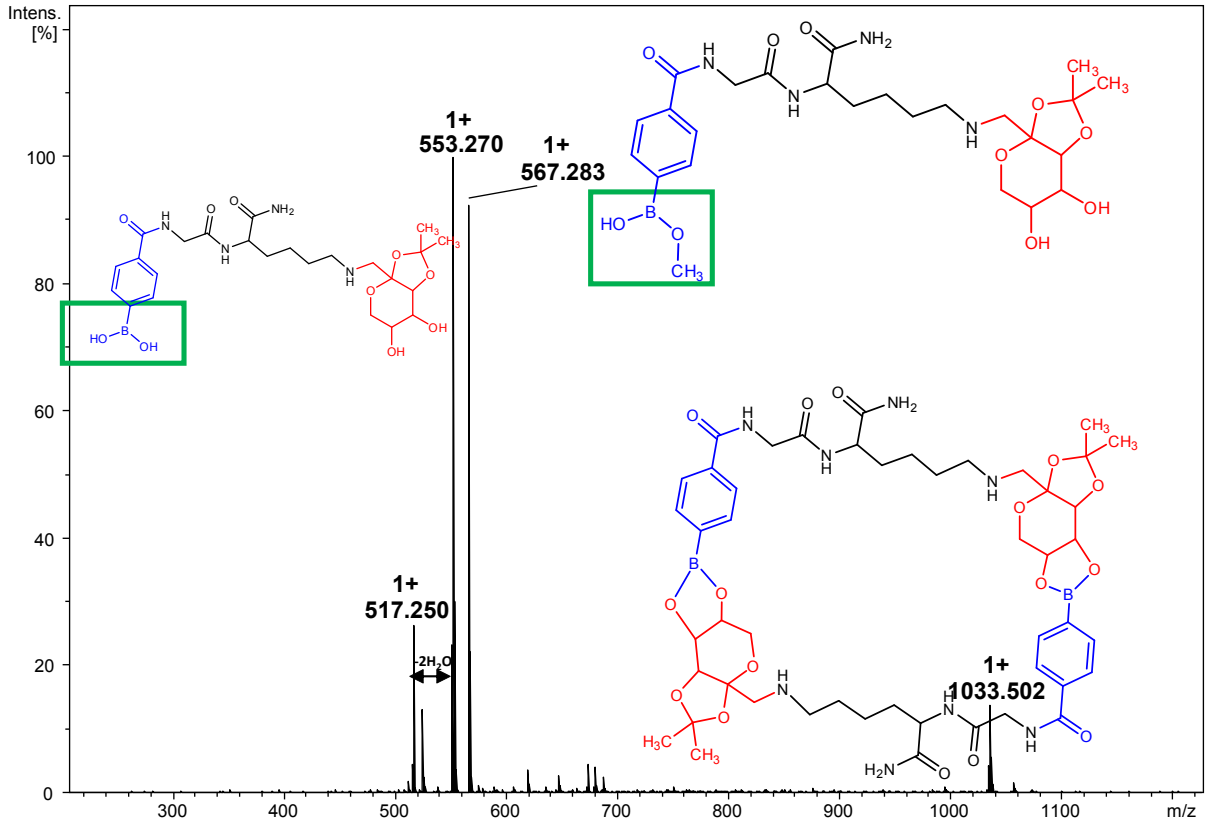

Fig. S12 ESI-MS spectrum of peptide PhB-Gly-Lys(Fru)-NH_2 (experiment performed in positive ion mode in solvent MeOH).

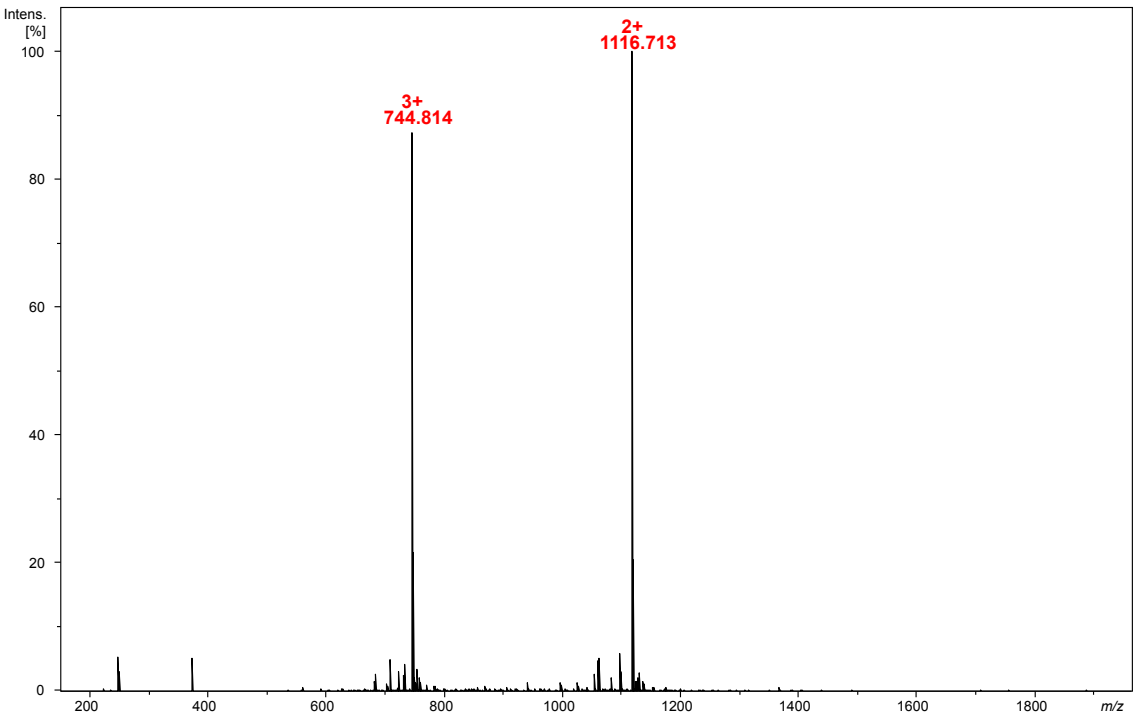

Fig. S13 ESI-MS spectrum of peptide Fru1PhB4 (experiment performed in positive ion mode in solvent MeOH).

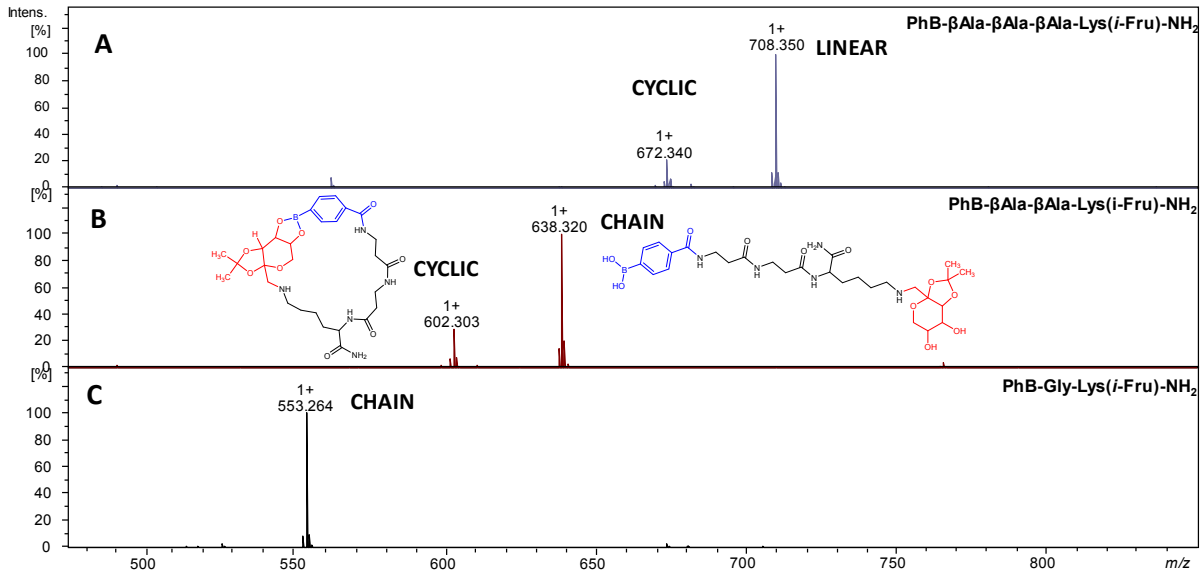

Fig. S14 ESI-MS spectra of model peptides: A – PhB-βAla-βAla-βAla-Lys(*i*-Fru)-NH_2; B – PhB-βAla-βAla-Lys(*i*-Fru)-NH_2; C – PhB-Gly-Lys(*i*-Fru)-NH_2; D – Fmoc-Lys(*i*-Fru)-OH.

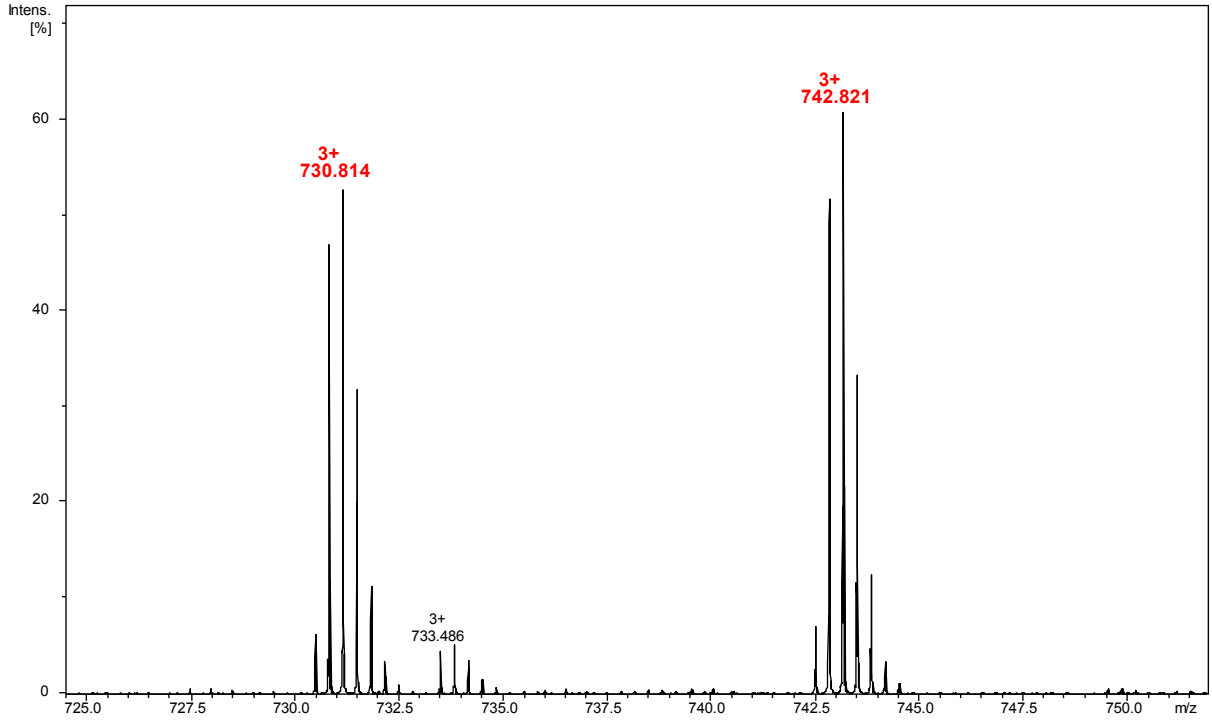

Fig. S15 ESI-MS spectrum of peptide PhB-KLALKLALK(Fru)ALKAALKLA-NH_2.

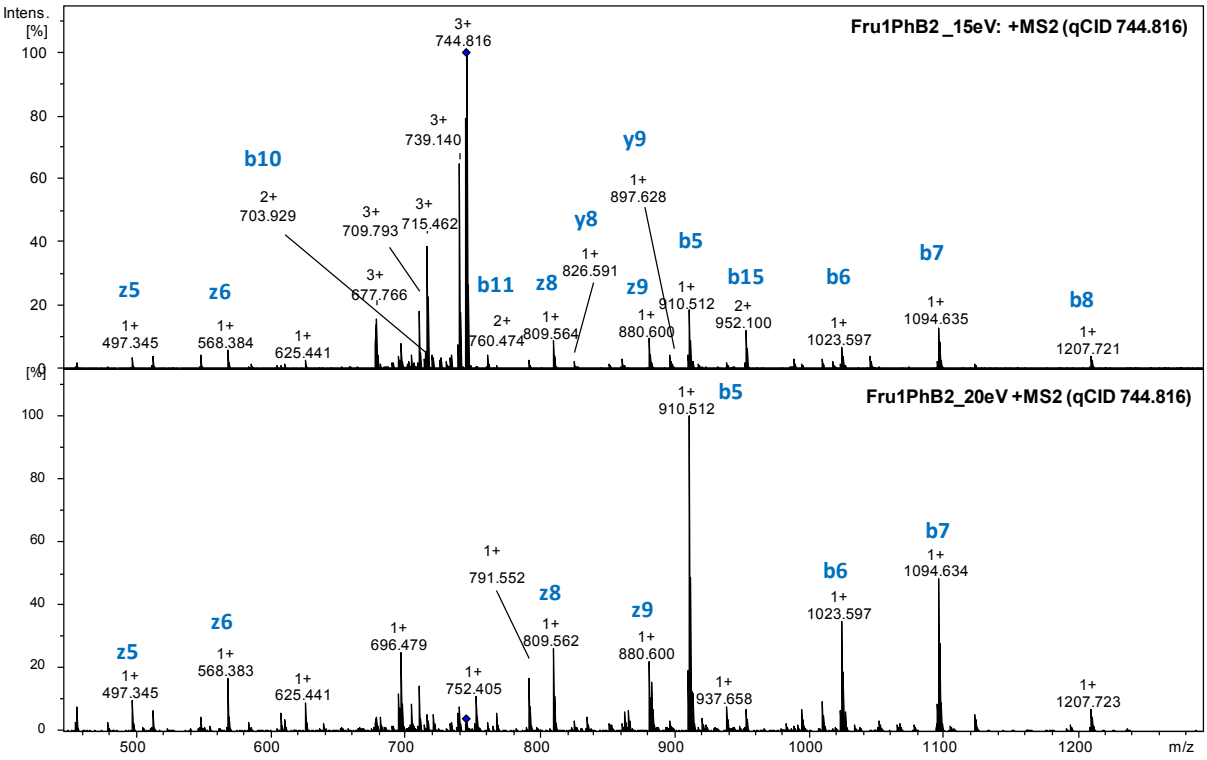

Fig. S16 ESI-MS/MS spectrum of peptide Fru1PhB2 (spectra were recorded for collision energy: 15eV and 18eV, parent ion: 744.816 *m/z*).

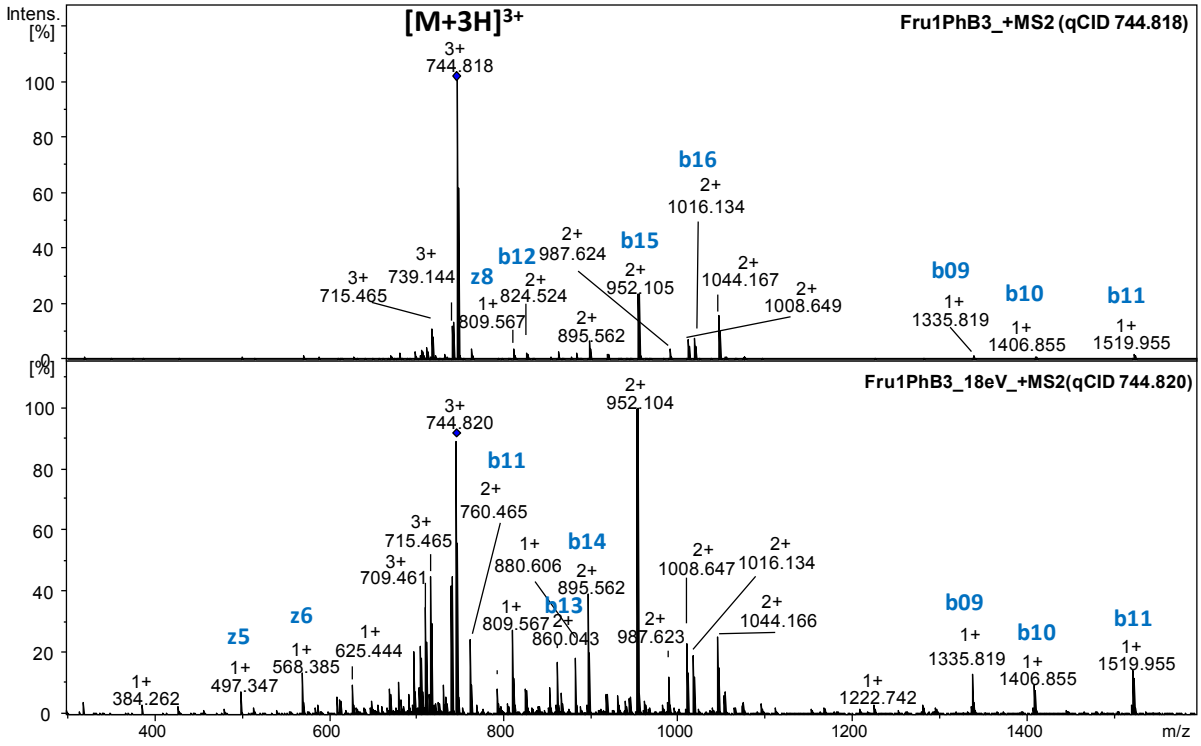

Fig. S17 ESI-MS/MS spectrum of peptide Fru1PhB3 (spectra were recorded for collision energy: 15eV and 18eV, parent ion: 744.816 *m/z*).

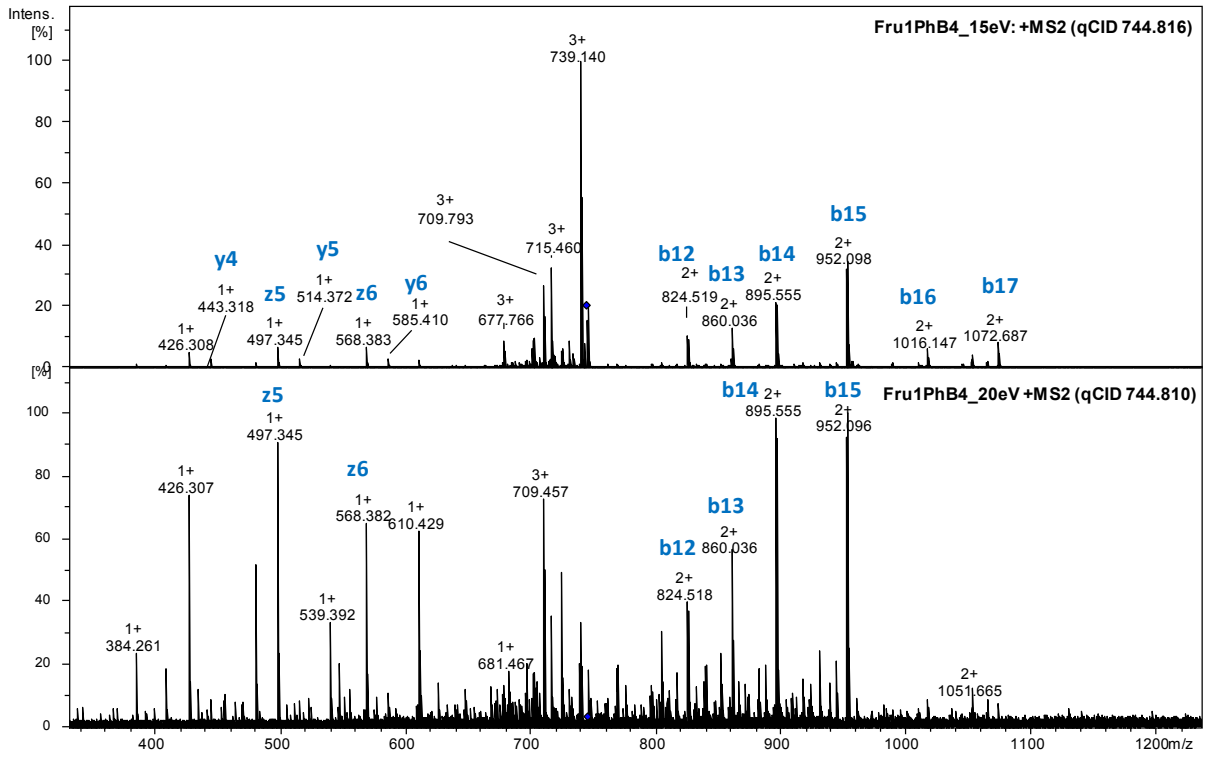

Fig. S18 ESI-MS/MS spectra of peptide Fru1PhB4 (spectra were recorded for collision energy: 15eV and 20eV, parent ion: 744.818 m/z).

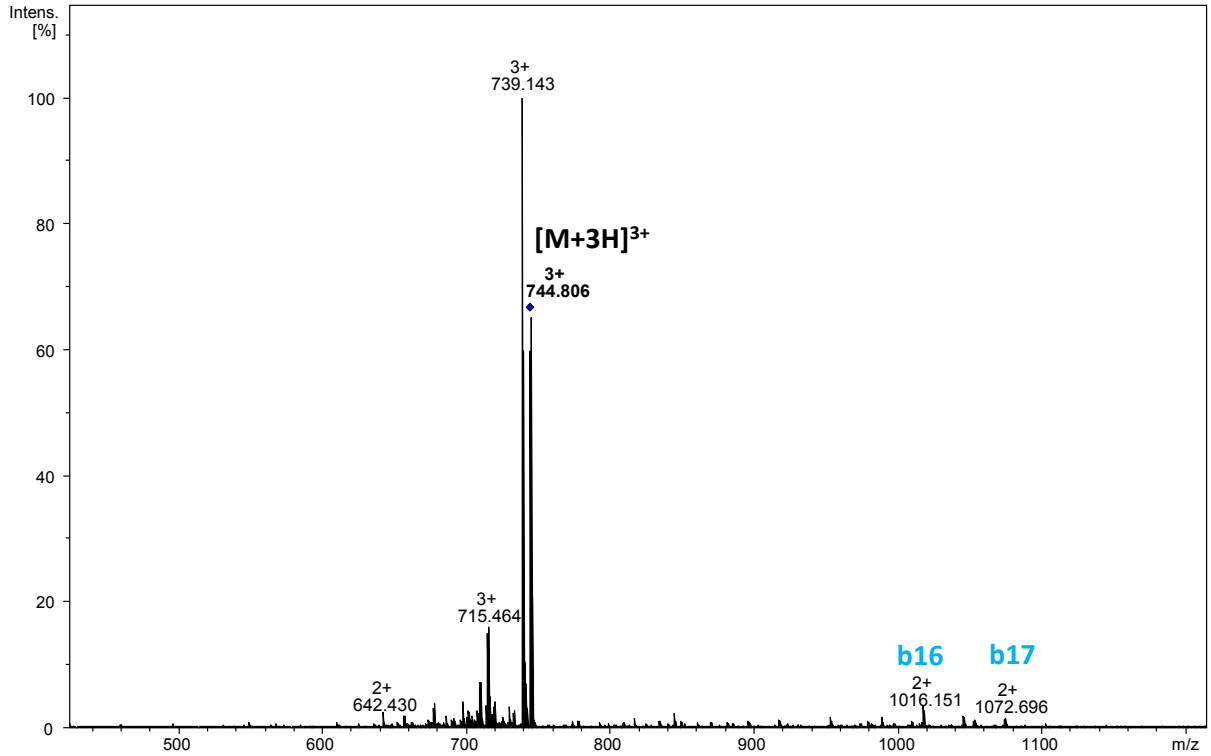

Fig. S19 ESI-MS/MS spectrum of peptide Fru1PhB5 (collision energy: 15eV; parent ion: 744.806 *m/z*).

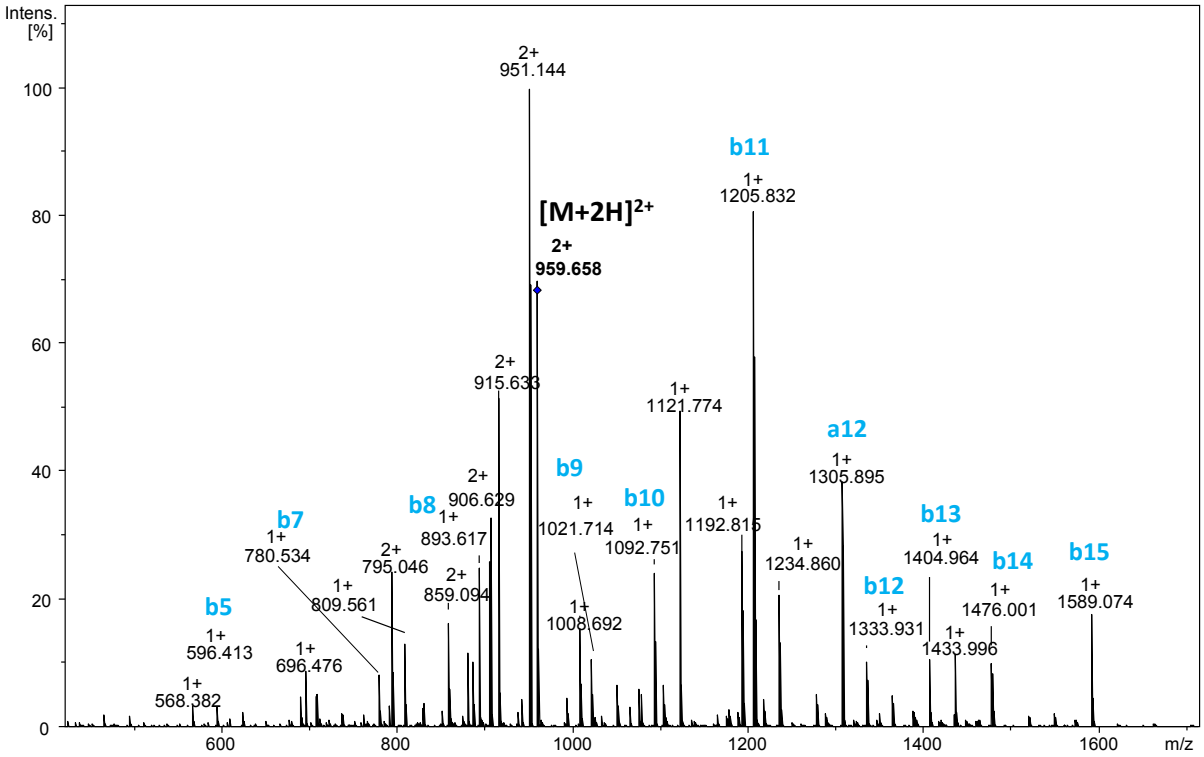

Fig. S20 ESI-MS/MS spectrum of peptide Ac-RNasaA*-NH2 (* C peptide sequence of RNasaA) (collision energy: 15eV; parent ion: 959.658 *m/z*).

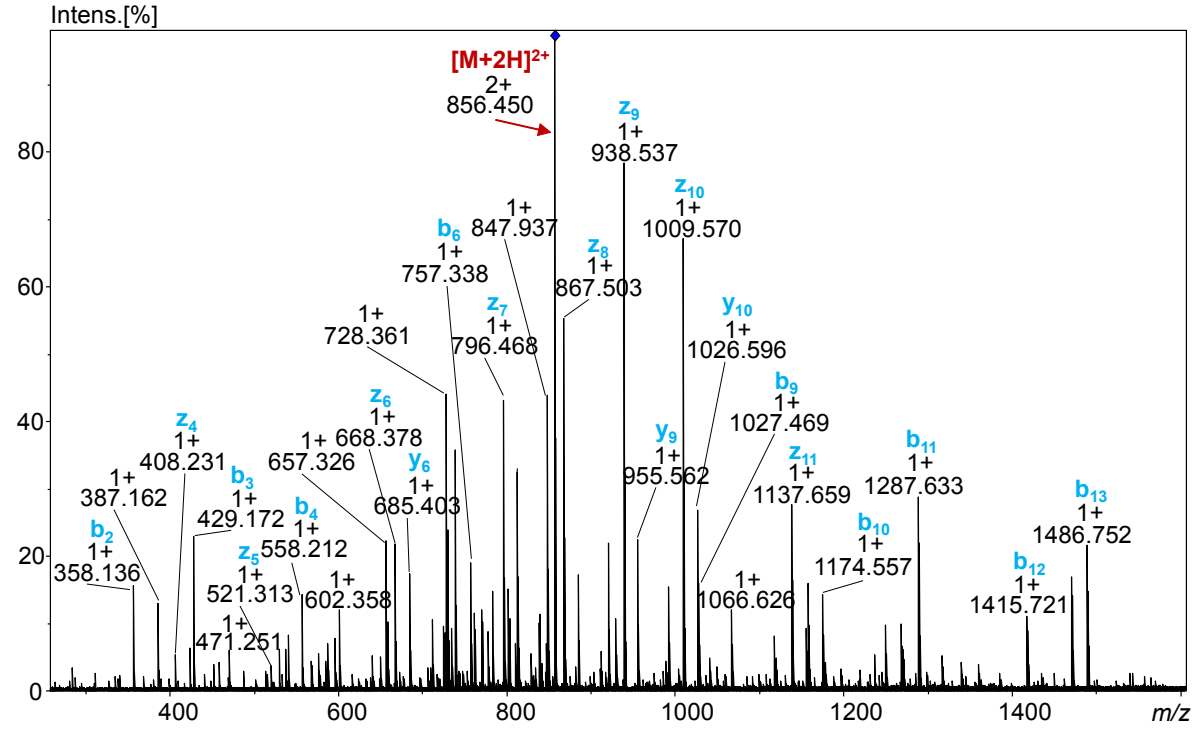

Fig. S21 ESI-MS/MS spectrum of peptide Ac-RNaseA* (* - C peptide sequence of RNaseA) (collision energy: 22eV; parent ion: 856.450 *m/z*).

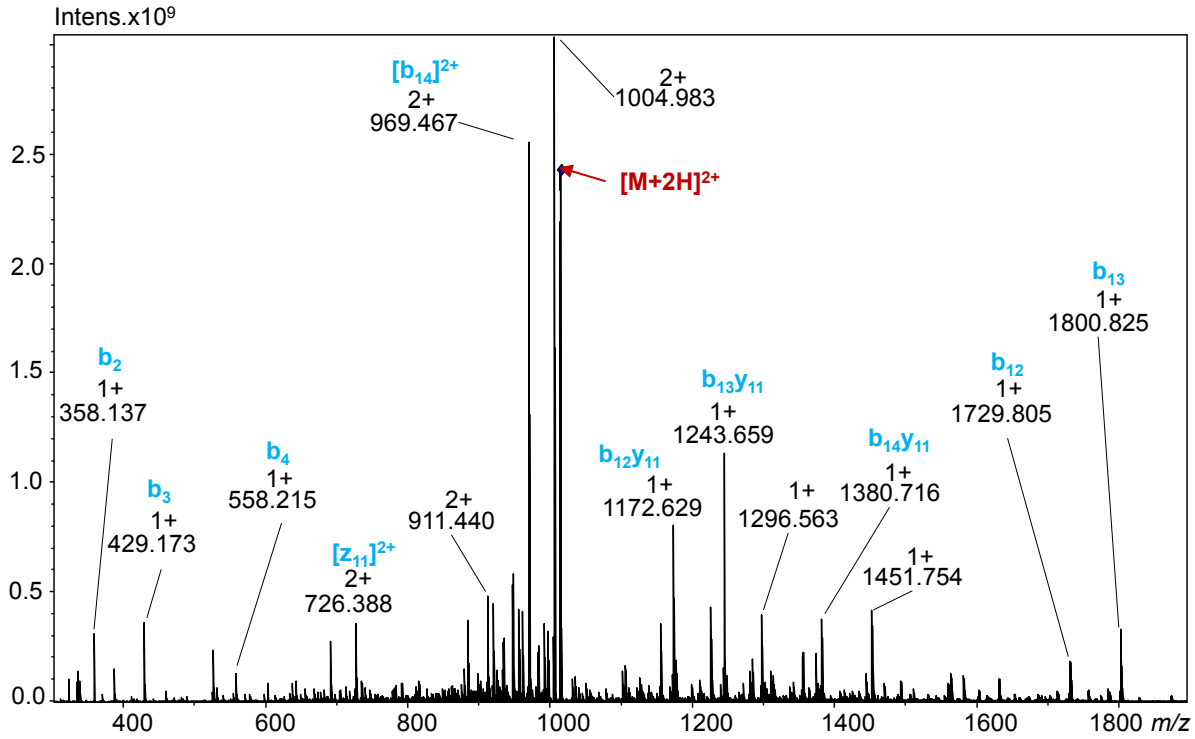

Fig. S22 ESI-MS/MS spectrum of peptide Fru1PhB3* (* - C peptide sequence of RNaseA) (collision energy: 30eV; parent ion: 1013.515 *m/z*).

5. CD analysis

Table S2 The list of peptides secondary structure contents.

Abbreviation	Helix [%]	Sheet [%]	Turn [%]	Other [%]
Ac-MAP	15.00	22.20	15.70	46.90
Fru1PhB2	22.00	16.40	15.70	45.70
Fru1PhB3	12.30	26.70	15.40	45.50
Fru1PhB4	26.90	14.00	16.60	42.40
Fru1PhB5	16.40	23.20	16.20	44.90

Table S3 The list of peptides melting temperature

Abbreviation	Melting Temperature (Tm)
Ac-MAP	72 ± 2ºC
Fru1PhB2	75 ± 2ºC
Fru1PhB3	70 ± 2ºC

Fru1PhB4	40 ± 2ºC
Fru1PhB5	60 ± 2ºC
Ac-RNaseA*	20± 2ºC
Fru1PhB3*	67 ± 2ºC

The analogue of C-terminal 15-peptide from pancreatic Ribonuclease A (RNaseA*) has been chosen as the model for a helical conformation stabilization by stapling. The all-hydrocarbon stapled analogue of this sequence was reported as the peptide with α-helical conformation stabilized by the stapling (Schafmeister CE, Po J, Verdine GL. An all-hydrocarbon cross-linking system for enhancing the helicity and metabolic stability of peptides, J Am Chem Soc 2000; 122: 5891–2). The choice of the sequence was dictated by well documented conformational preferences of the peptide. The conformational stabilities of Ac-RNaseA*-NH2 (Ac-EWAEKAAAKFLKAHA-NH2), and its analogue, Fru1PhB3* (Ac-EWAEcyclo(K(i-Fru)AAAKFLK(PhB))AHA-NH2), containing the stapling motif between Lys-5 and Lys-12 residues, were analyzed by temperature-variable CD (circular dichroism) measurements of spectra in near UV, with temperature range starting at 5°C up to 95°C for the stapled analogue. At room temperature, the unmodified Ac-RNaseA* shows CD spectrum characteristic for peptides with an unordered conformation, with strong negative band at about 200 nm (**Fig. S23**). However, the analysis of the peptide at lower temperature indicated preferences towards creating a α-helical ordered structure by a part of the sequence. With increasing temperature from 5 to 35°C, we observed the hypsochromic shift of the negative band from 202.4 to 200 nm, accompanied with decreasing intensities of the positive band at about 190 nm and the negative band at 220 nm. These changes correlate well with an expected disordering of the peptide during heating. For such short peptides, "the melting of a conformation" may be observed as a continuous process. Nonetheless, by analyzing changes in intensity of the band at 220 nm, we found the melting point of the helical conformation (participated in the average structure) at about 20°C (**Fig. S24**).

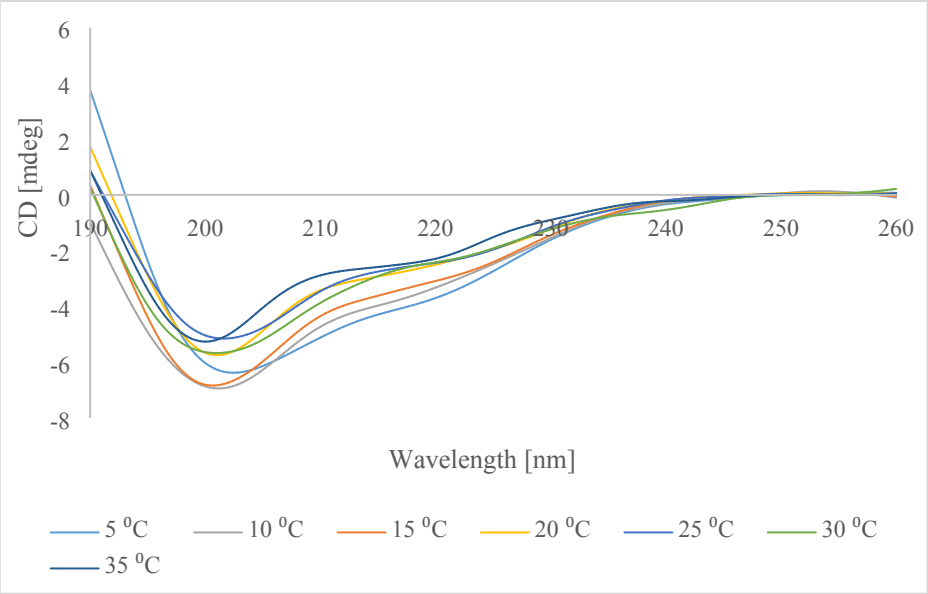

Fig. S23 CD spectra of Ac-RNaseA* at different temperatures

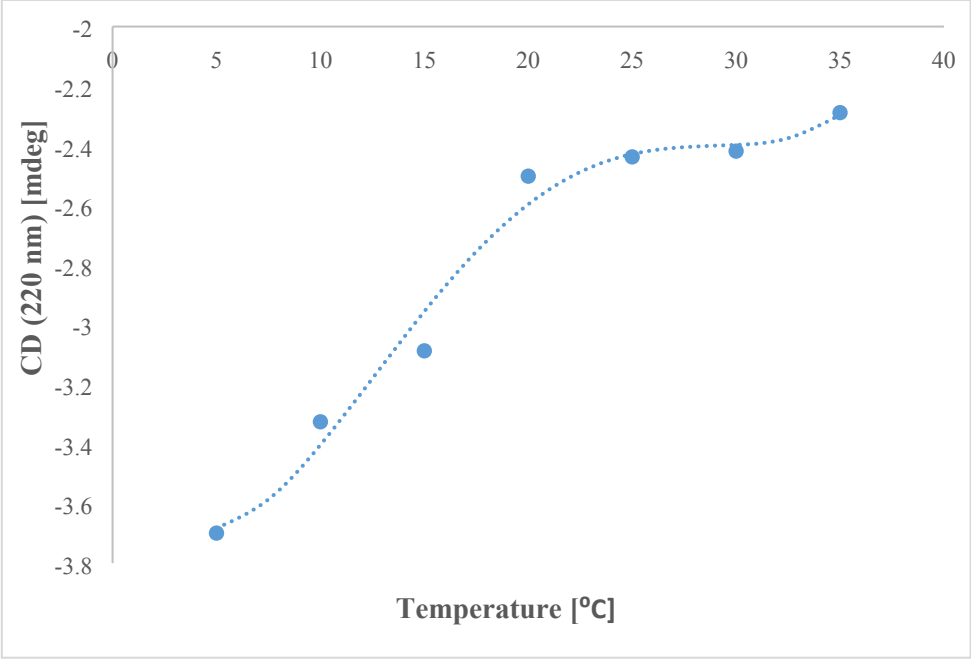

Fig. S24 Circular dichroism intensity at 220 nm in the function of temperature for Ac-RNase*. Melting curve.

The stapled analogue, Fru1PhB3*, has a high content of α-helical conformation. The two negative bands with comparable intensities at about 204 nm and 220 nm, accompanied by strong positive band at 190 nm or lower wavelengths, are characteristic of this type of structure. In general, decreasing of the bands intensities is continuous with the temperature rise. During the increase in temperature from 5 to 60°C, we did not observe any significant changes in the shape and the location of main bands of the CD spectrum (**Fig. S25**). At temperatures above 60°C, the intensity of the positive band of the exciton doublet of peptide bond chromophores starts to decrease more quickly, reaching aplateau at about 75°C. This behavior corresponds with an expected decay of the helical structures content. We found the melting point of the helical conformation at about 65-70°C (**Fig. S26**). However, this process

is accompanied by the batochromic shits of the negative band from 204 nm to 207 nm, indicating changes in conformation rather than a complete disordering of the structure. Even at temperatures higher than 90°C, the shape of the CD spectra shows some contributions of helical and beta conformations. The linker between Lys(i) and Lys(i-7) residues in Fru1PhB3* acts to trigger conformational changes, favoring a formation of a kind of loop stabilizing, probably by antiparallel hydrogen bonds pattern in a β-hairpin-like motif that was observed by Zhao et al. (ChemBiochem., 2016, 17(15), 1416-1420)

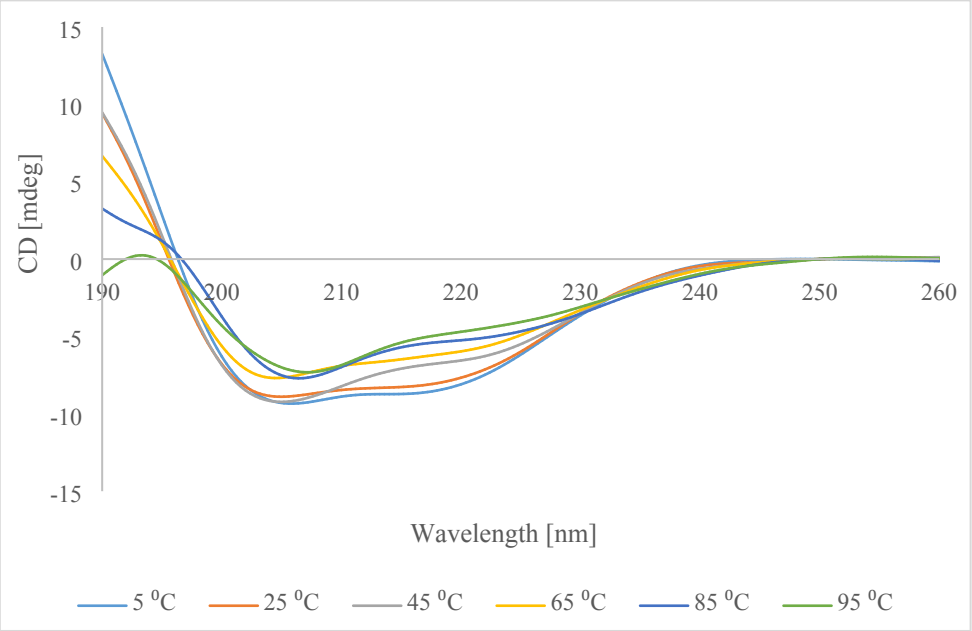

Fig. S25 CD spectra of Fru1PhB3* at different temperatures

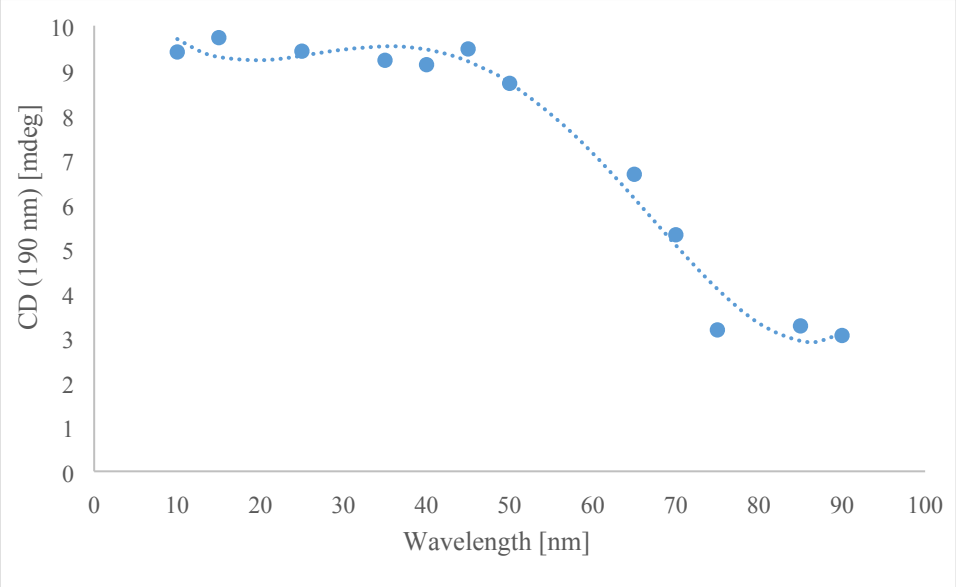

Fig. S26 Circular dichroism intensity at 190 nm in the function of temperature for Fru1PhB*. Melting curve.

Summarizing the results obtained from CD analysis, we can conclude that stapled peptide Fru1PhB3* is more stable than non-modified analogue.

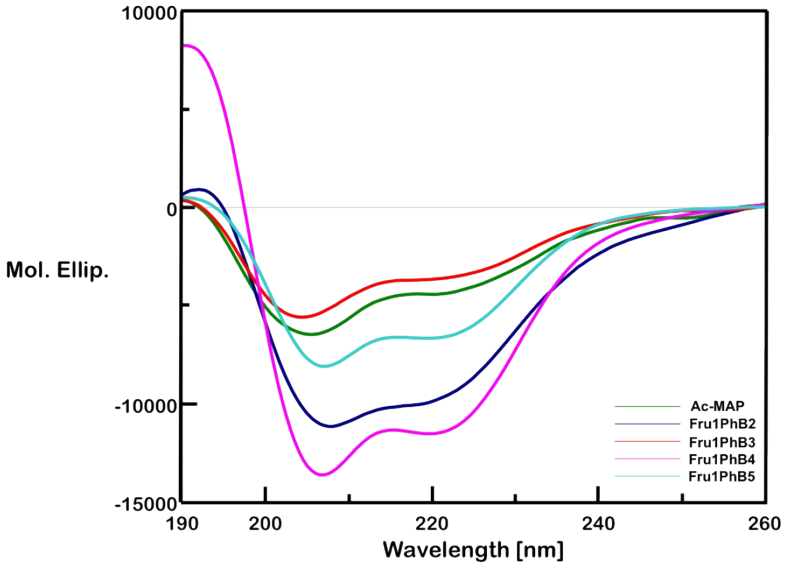

Fig.S27 Far-UV CD measurements of Ac-MAP, Fru1PhB2, Fru1PhB3, Fru1PhB4 and Fru1PhB5

6. NMR spectra

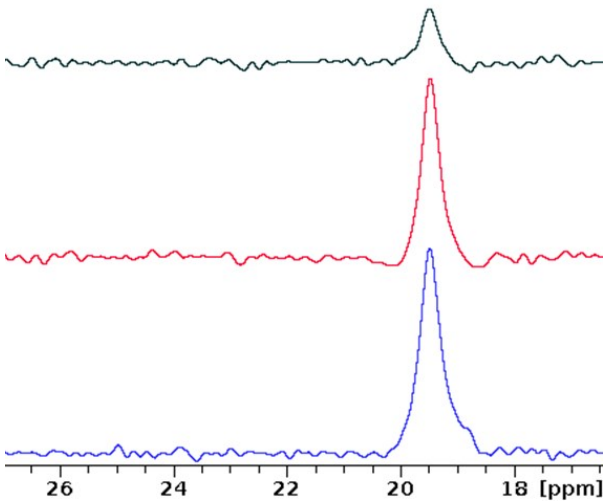

Fig. S28 The ^{11}B NMR spectra of the 3 samples, as follows: Fru1PhB3 (black line), Fru1PhB4 (red line), and Fru1PhB5 (blue line), respectively.

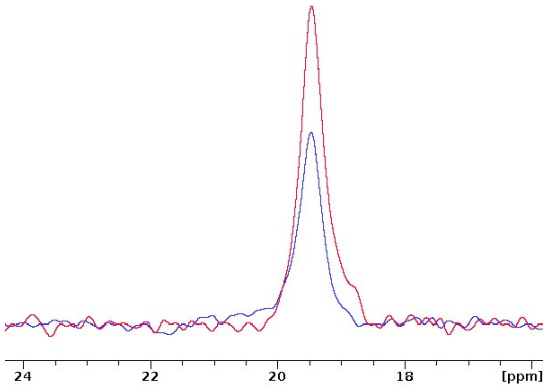

Fig. S29 The ^{11}B NMR spectra of peptide-free ~~Ac-MAP~~ PhB-Gly-Lys(*i*-Fru)-NH_2 sample (blue line) and Fru1PhB5 (red line).

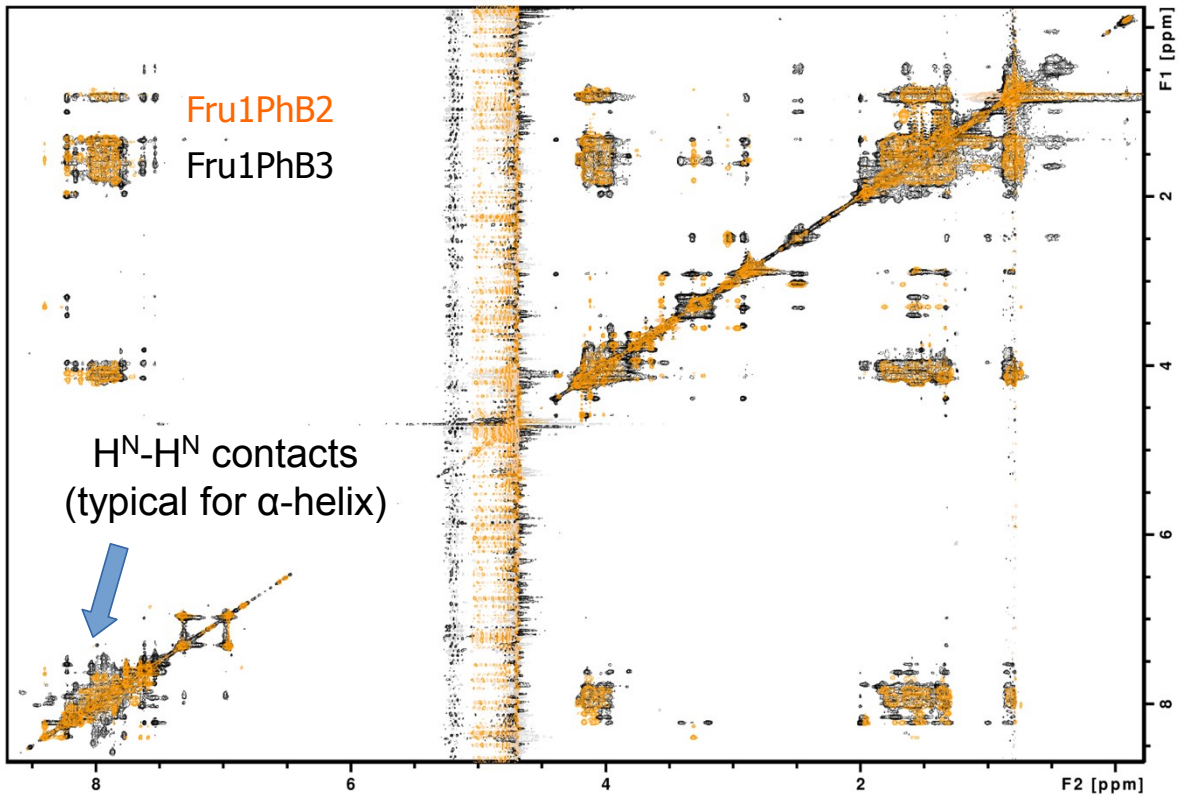

Fig. S30 2D ^{1}H-^{1}H-NOESY (200 ms mixing time) NMR spectrum for Fru1PhB2 (orange) and Fru1PhB3 (black).

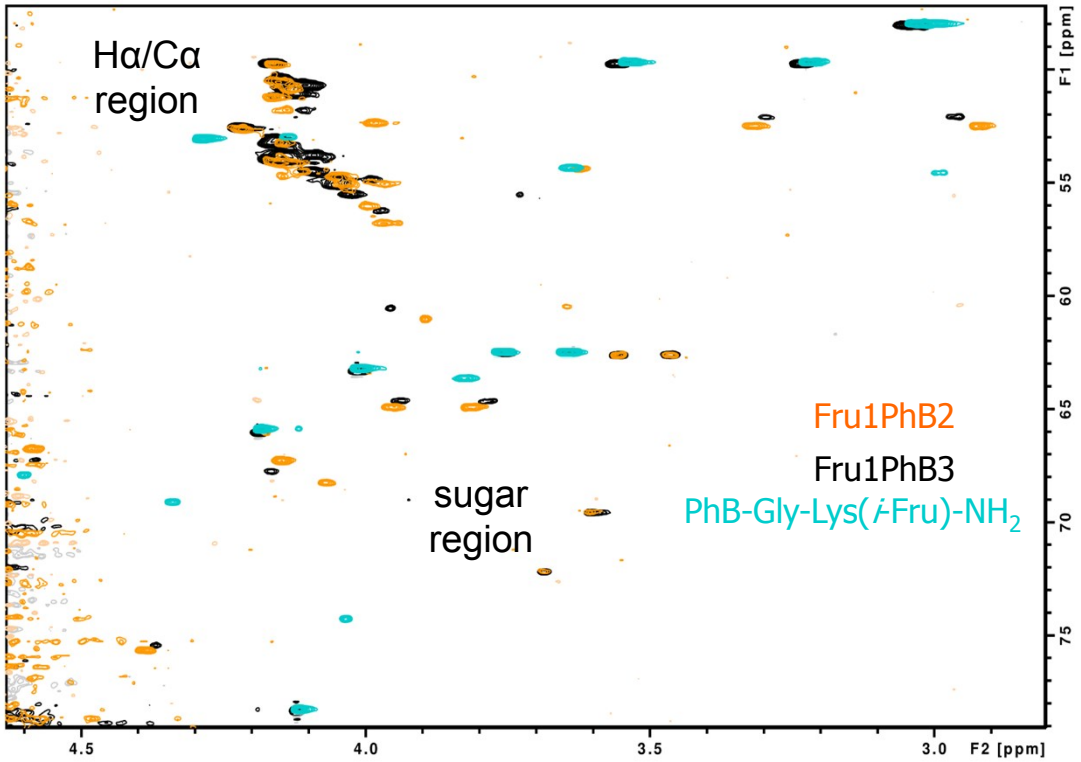

Fig. S31 The overlay of 2D ^{1}H-^{13}C HSQC NMR spectra for PhB-Gly-Lys(*i*-Fru)-NH_2 (cyan), Fru1PhB2 (orange) and Fru1PhB3 (black). Only the H/C alpha and sugar region is shown.

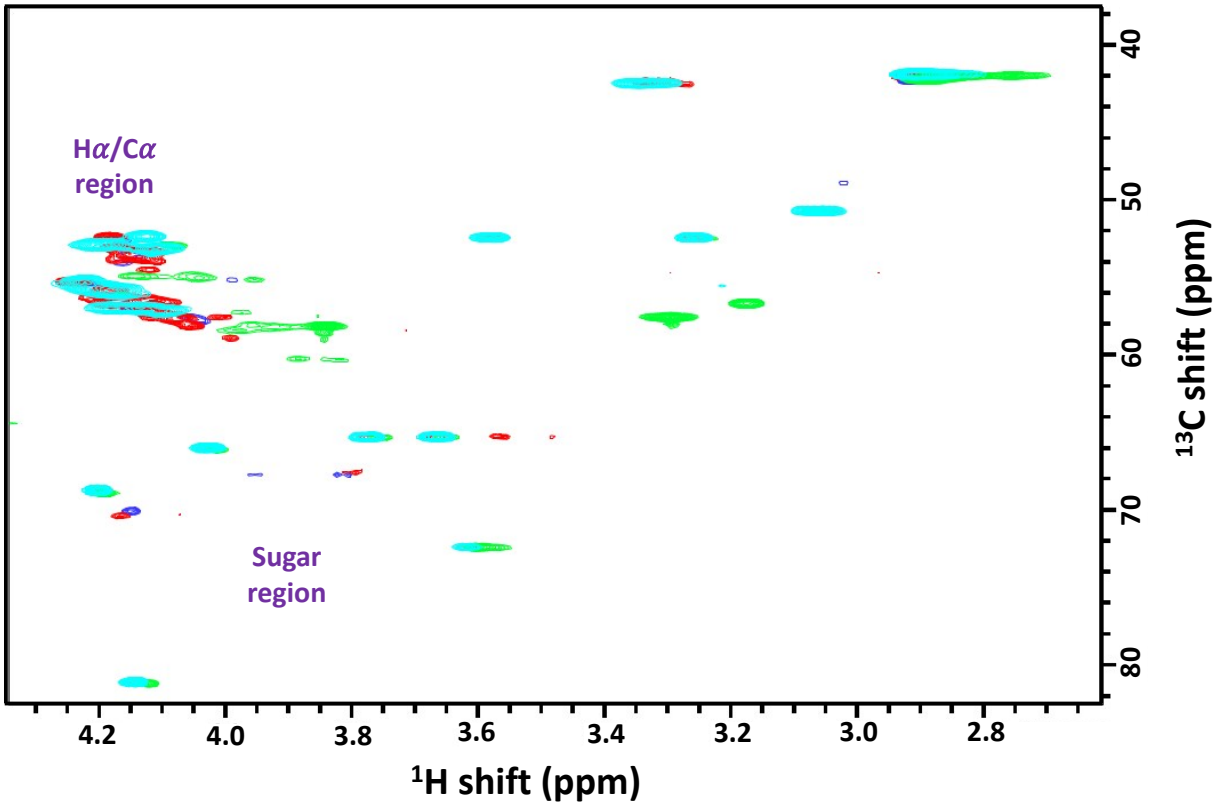

Fig. S32 ^{1}H – ^{13}C HSQC stacked plot of Fru1PhB2, Fru1PhB3, Fru1PhB4, and Fru1PhB5 spectra, highlighting the sugar region

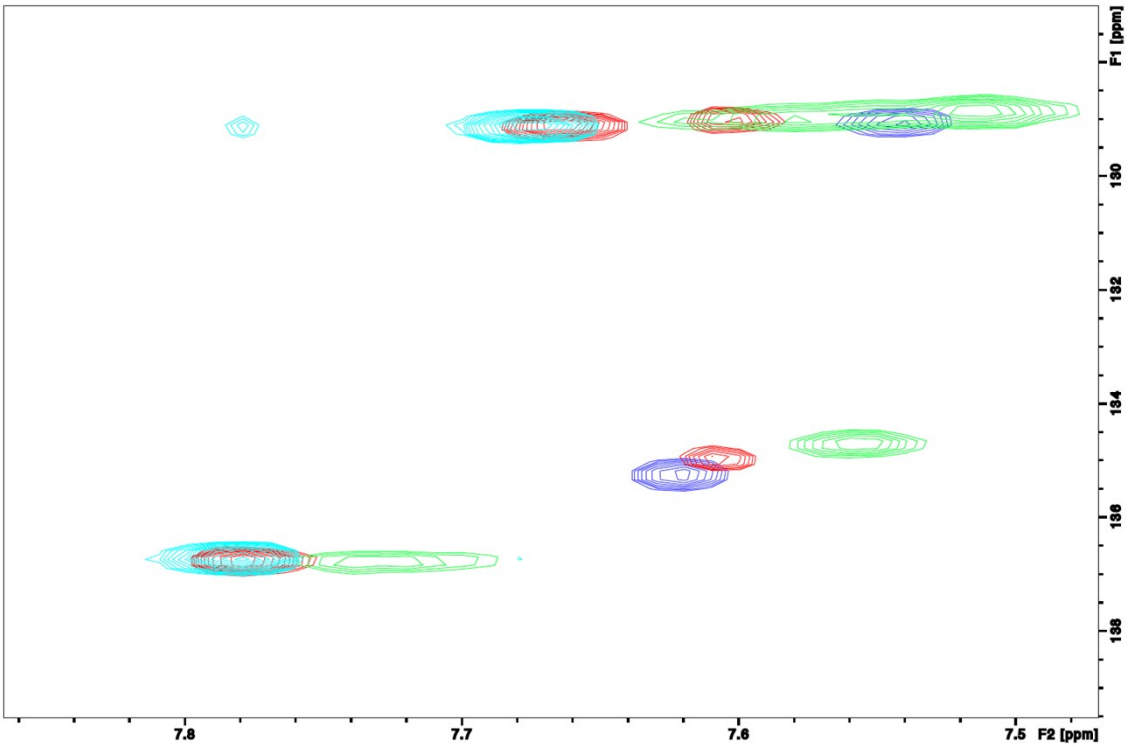

Fig. S33 ^{1}H – ^{13}C HSQC stacked plot of Fru1PhB2, Fru1PhB3, Fru1PhB4, and Fru1PhB5 spectra.

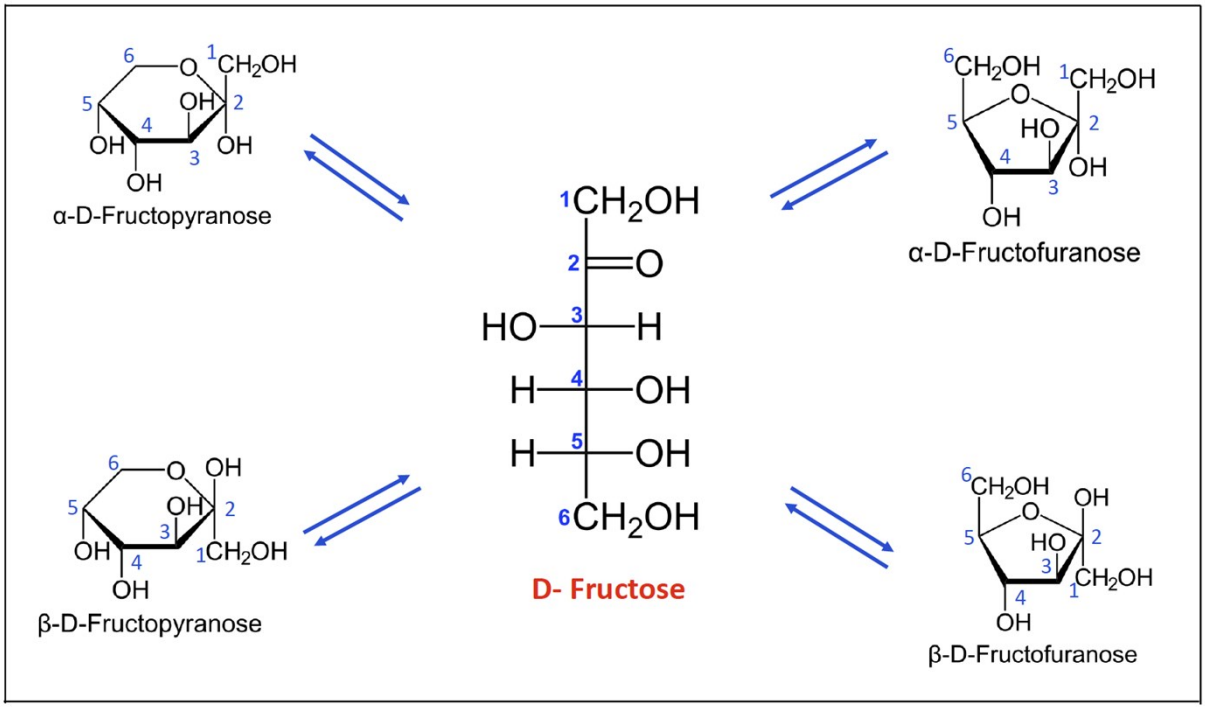

Scheme S1 Equilibria for the D-fructose-aminoacids in D_2O solution.

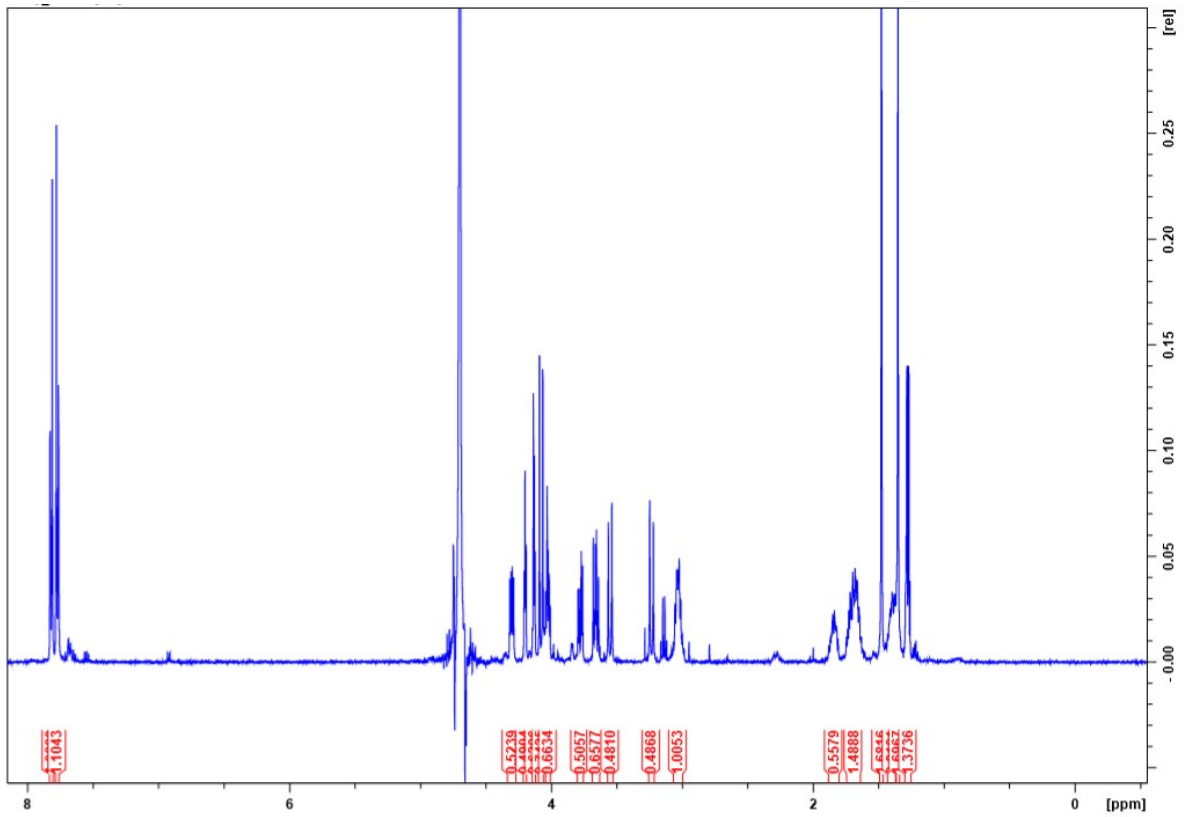

Fig. S34 ^{1}H spectrum of PhB-Gly-Lys(*i*-Fru)-NH_2.

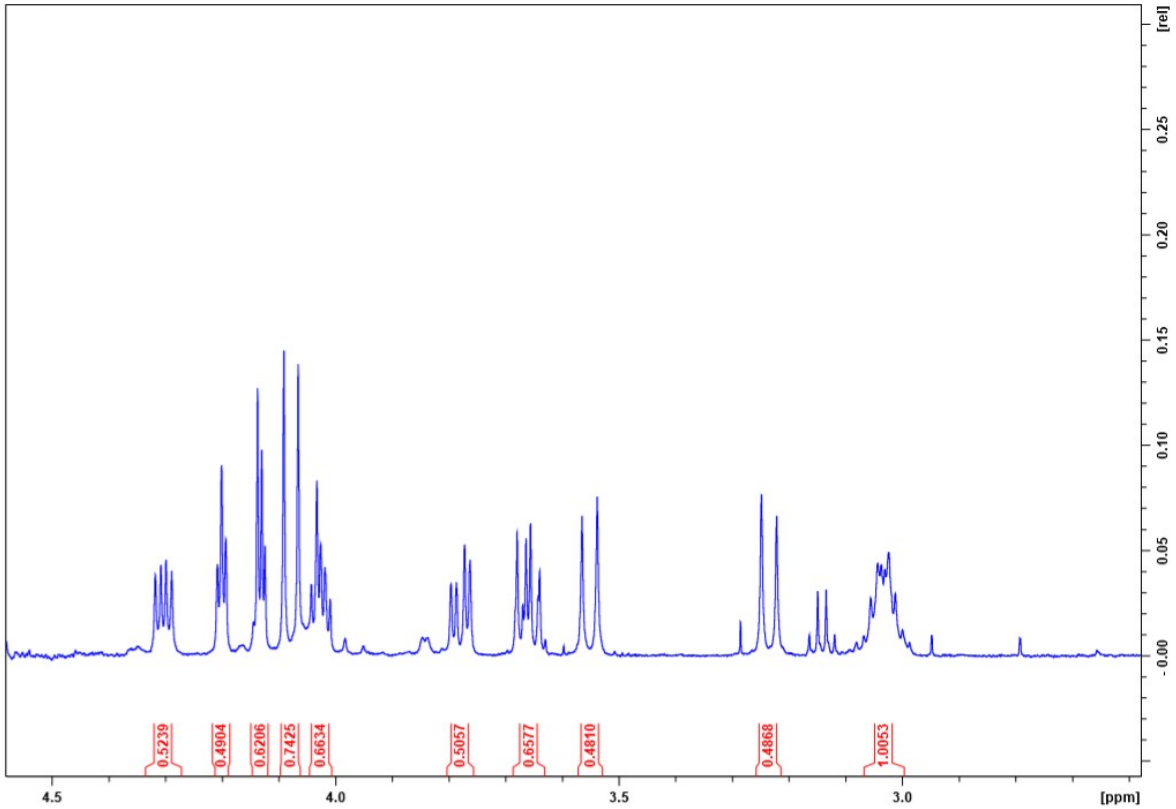

Fig. S35 ^{1}H spectrum (zoom of sugar region) of PhB-Gly-Lys(*i*-Fru)-NH_2

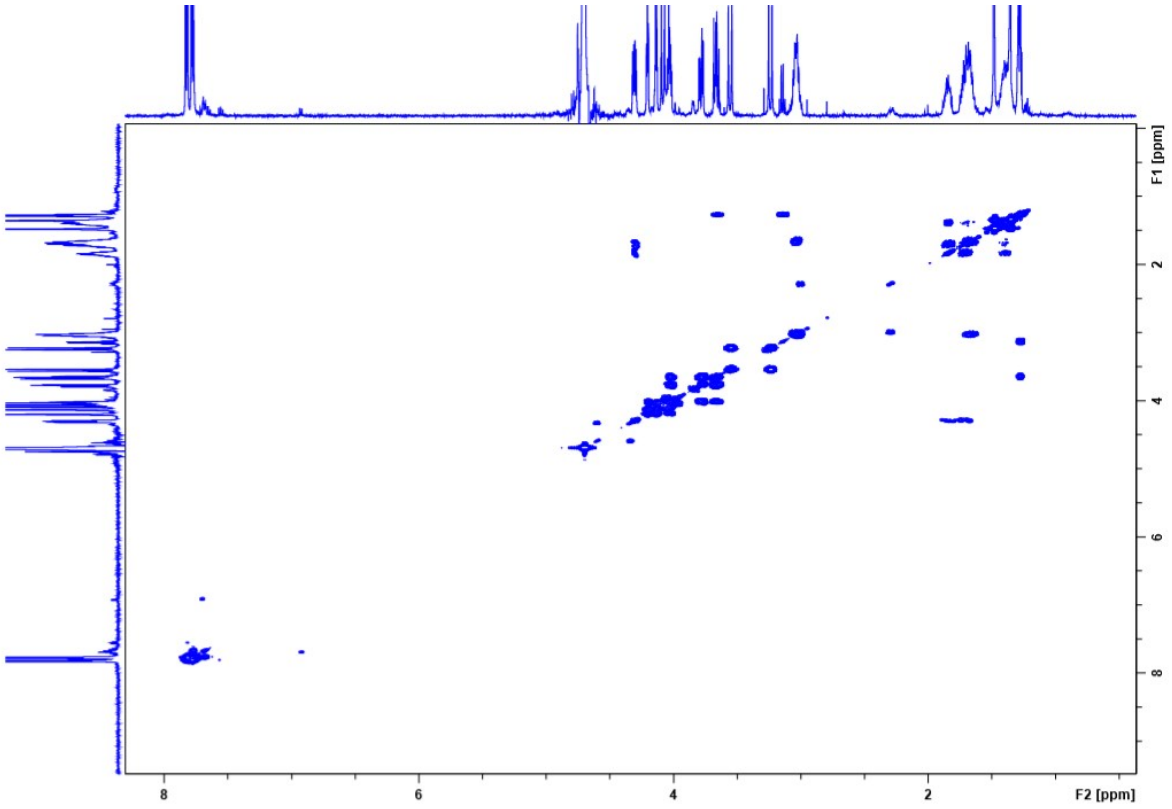

Fig. S36 COSY spectrum of PhB-Gly-Lys(*i*-Fru)-NH_2

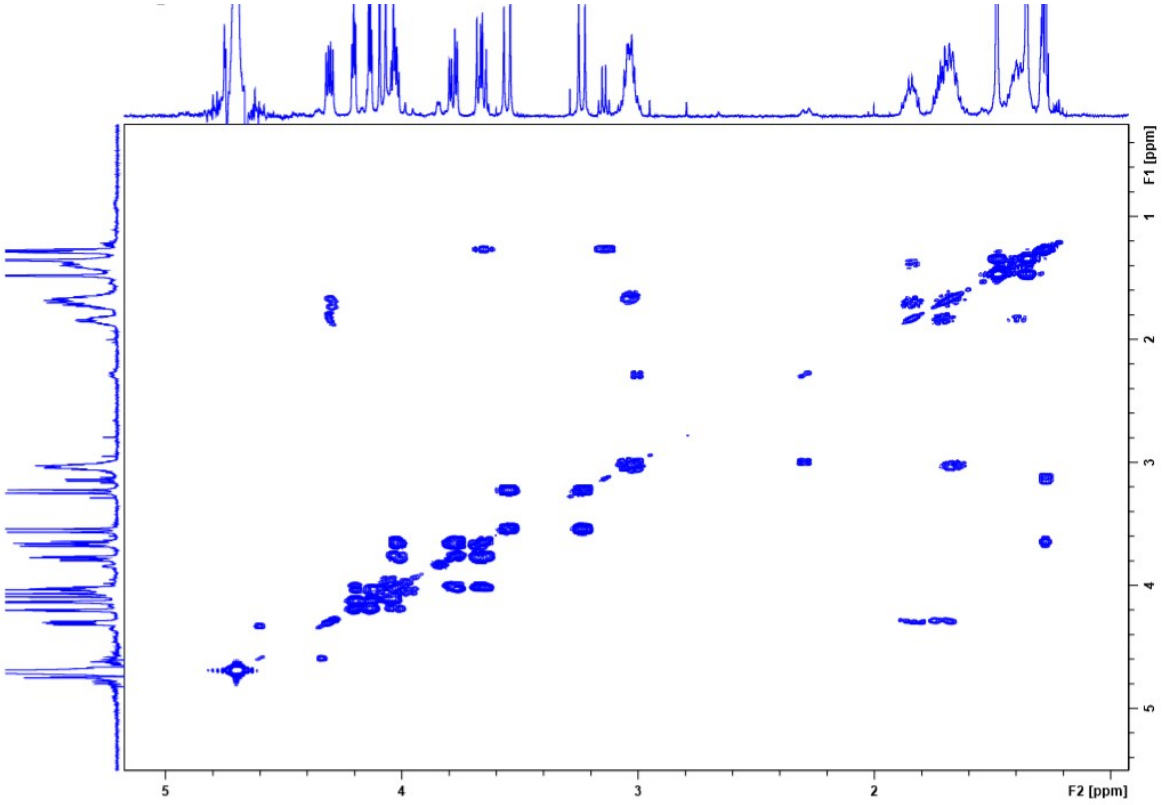

Fig. S37 COSY (zoom of sugar region) of PhB-Gly-Lys(*i*-Fru)-NH_2

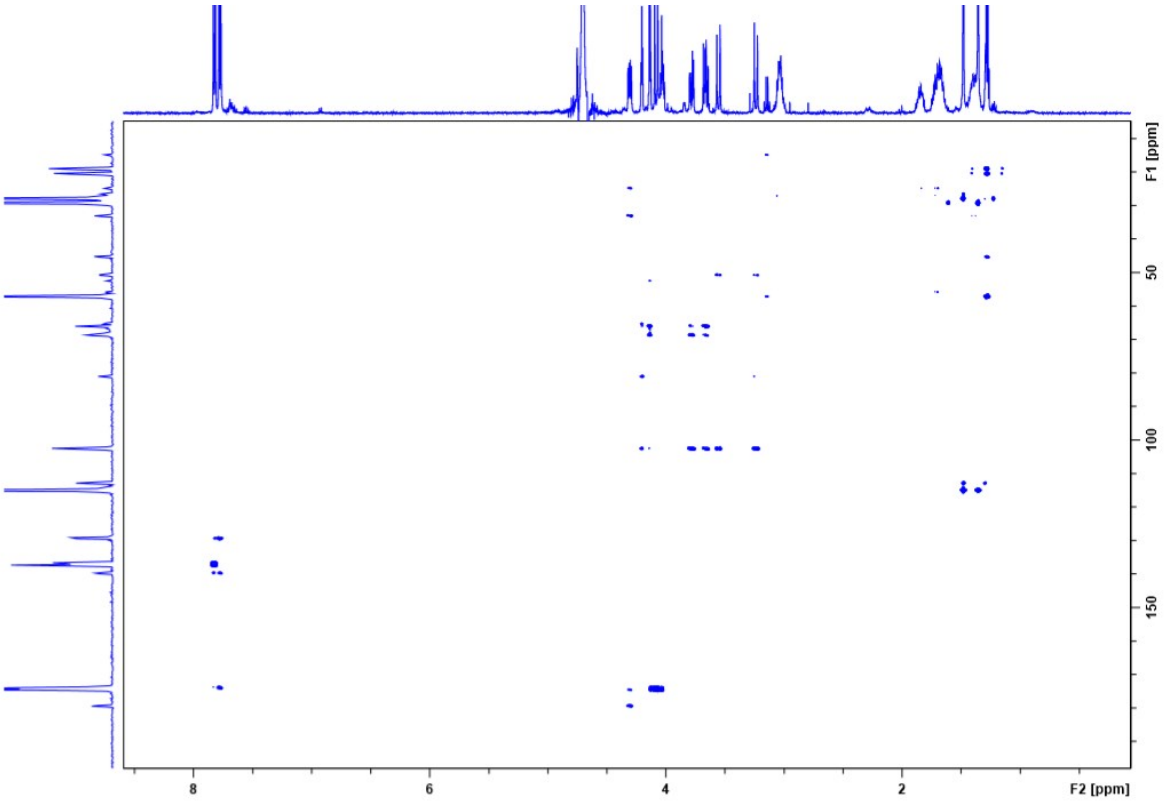

Fig. S38 HMBC spectrum of PhB-Gly-Lys(*i*-Fru)-NH_2

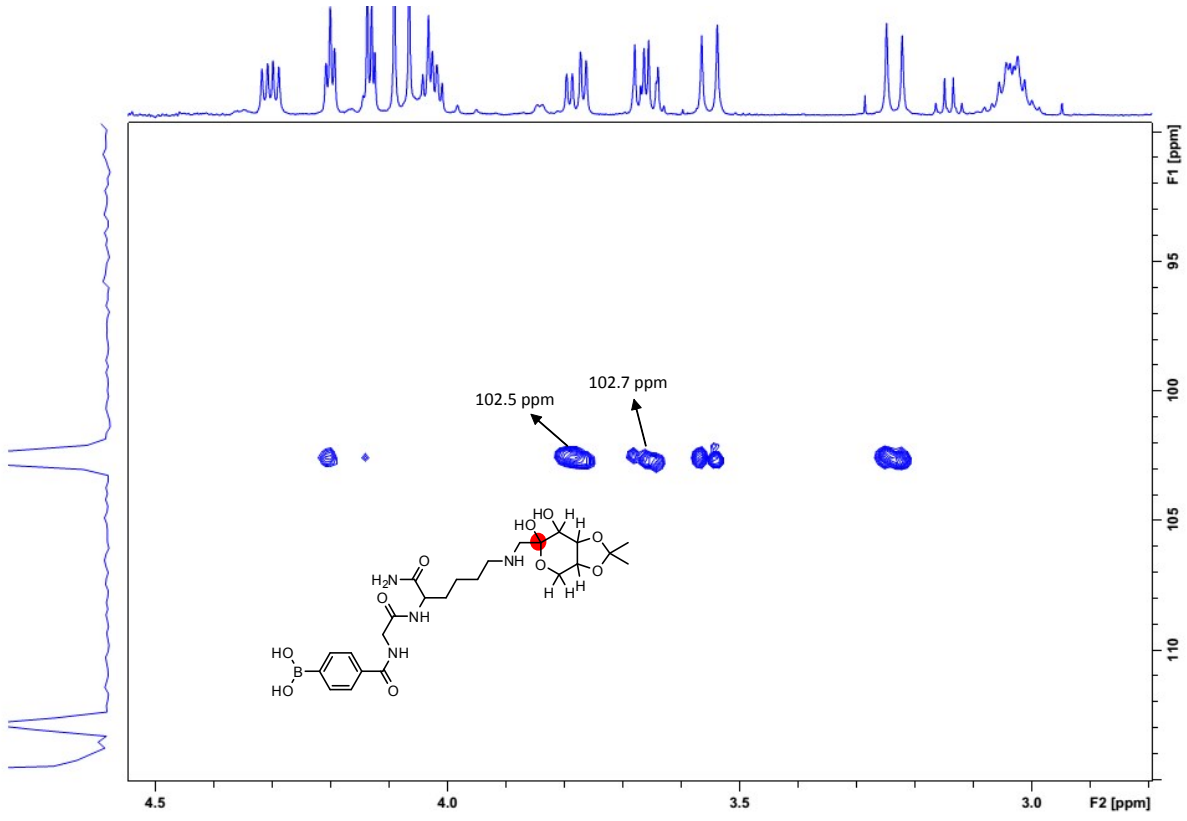

Fig. S39 HMBC spectrum (zoom of sugar region C2) of PhB-Gly-Lys(*i*-Fru)-NH_2

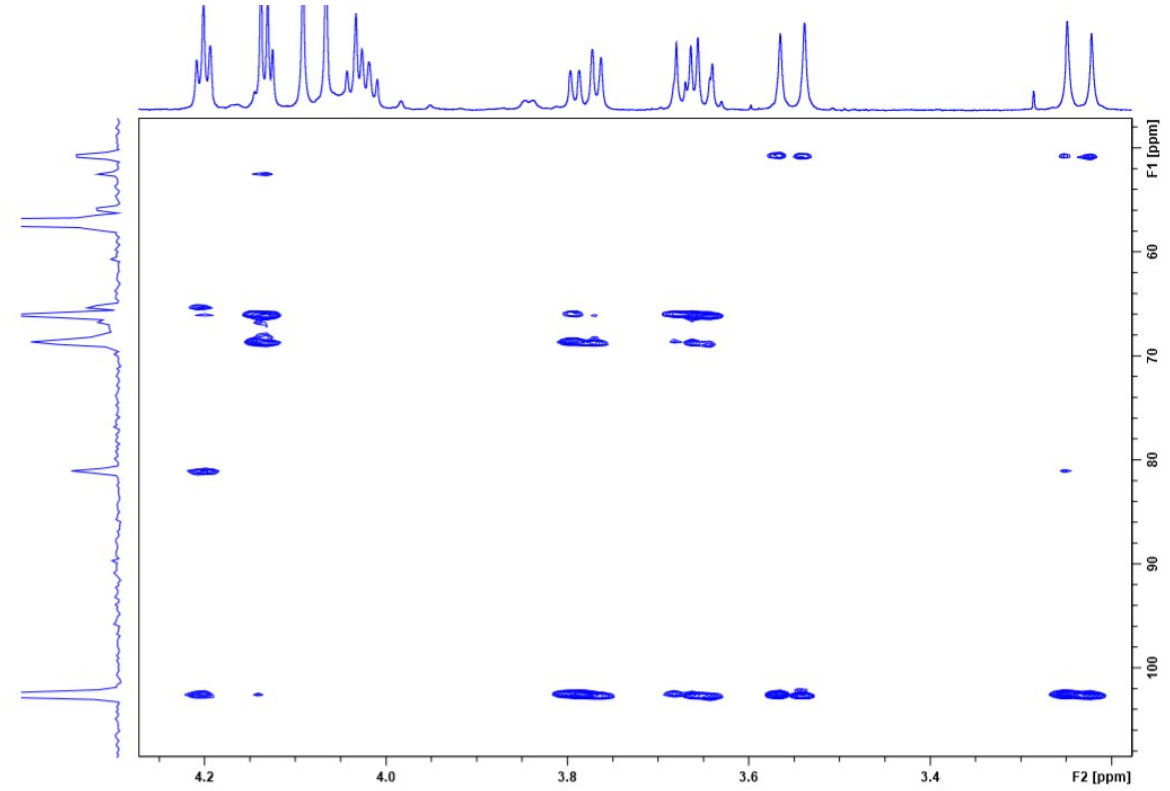

Fig. S40 HMBC spectrum (zoom of sugar region) of PhB-Gly-Lys(*i*-Fru)-NH_2

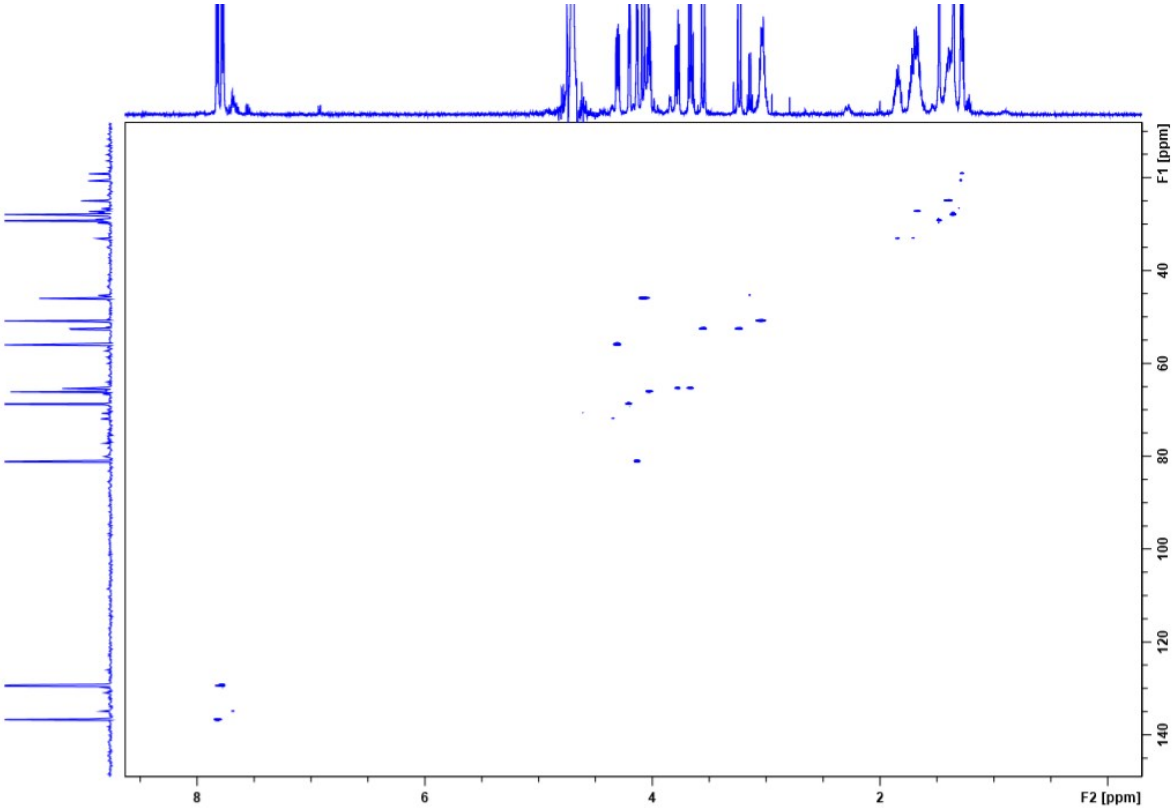

Fig. S41 HSQC spectrum of PhB-Gly-Lys(*i*-Fru)-NH_2

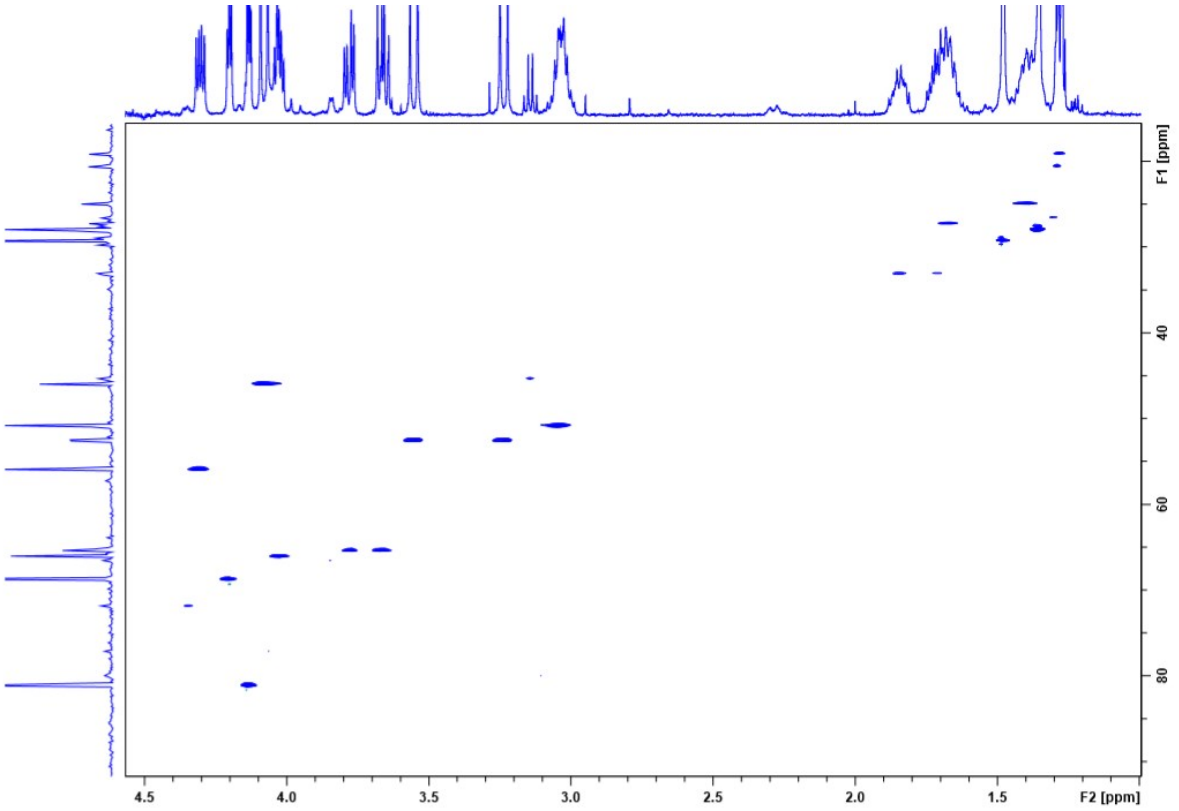

Fig. S42 HSQC spectrum (zoom of sugar region) of PhB-Gly-Lys(*i*-Fru)-NH_2

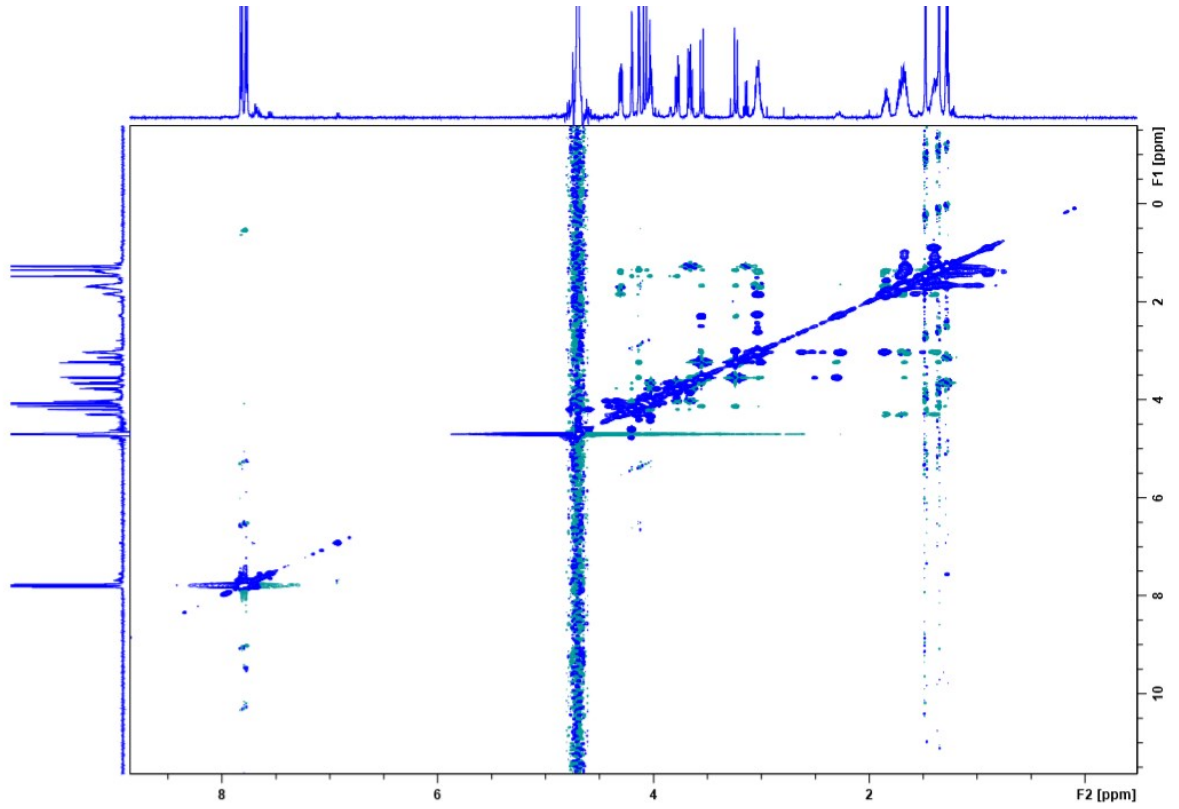

Fig. S43 NOESY spectrum of PhB-Gly-Lys(*i*-Fru)-NH_2

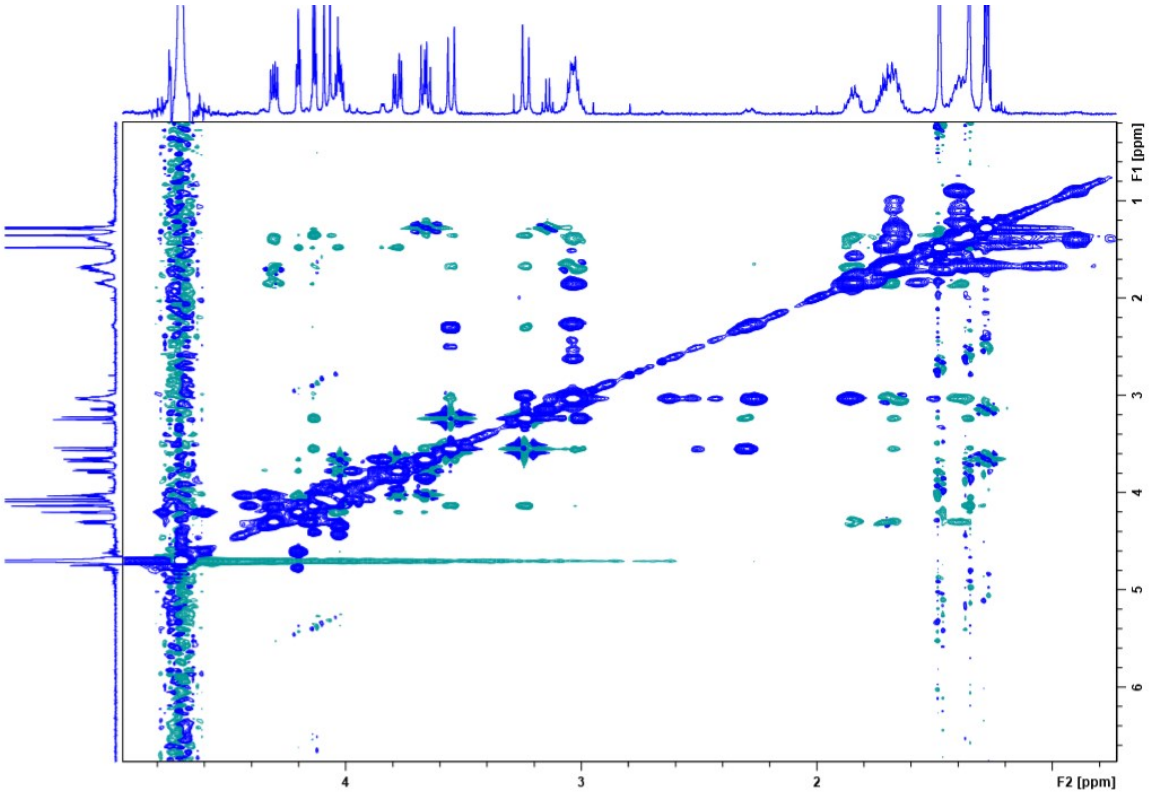

Fig. S44 NOESY spectrum (zoom of sugar region) of PhB-Gly-Lys(*i*-Fru)-NH_2

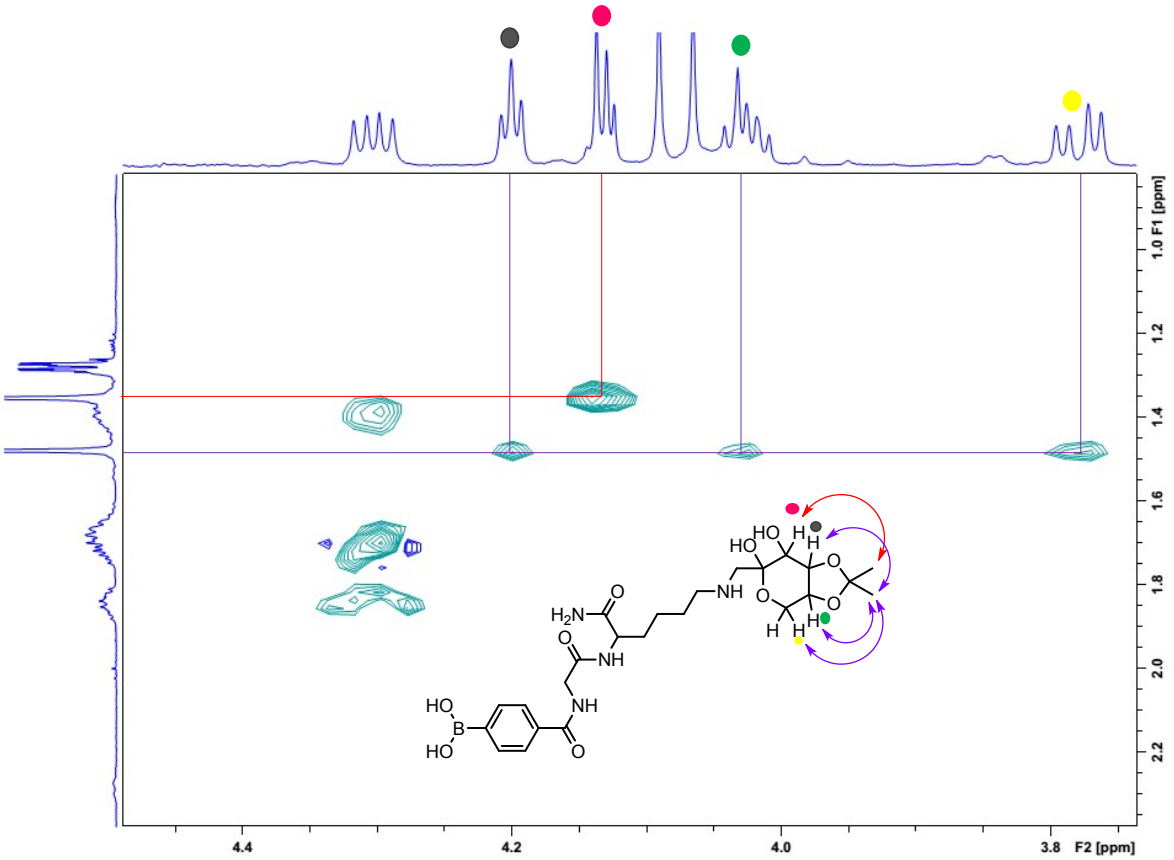

Fig. S45 NOESY spectrum (zoom of sugar region; isopropyliden group) of PhB-Gly-Lys(*i*-Fru)-NH_2

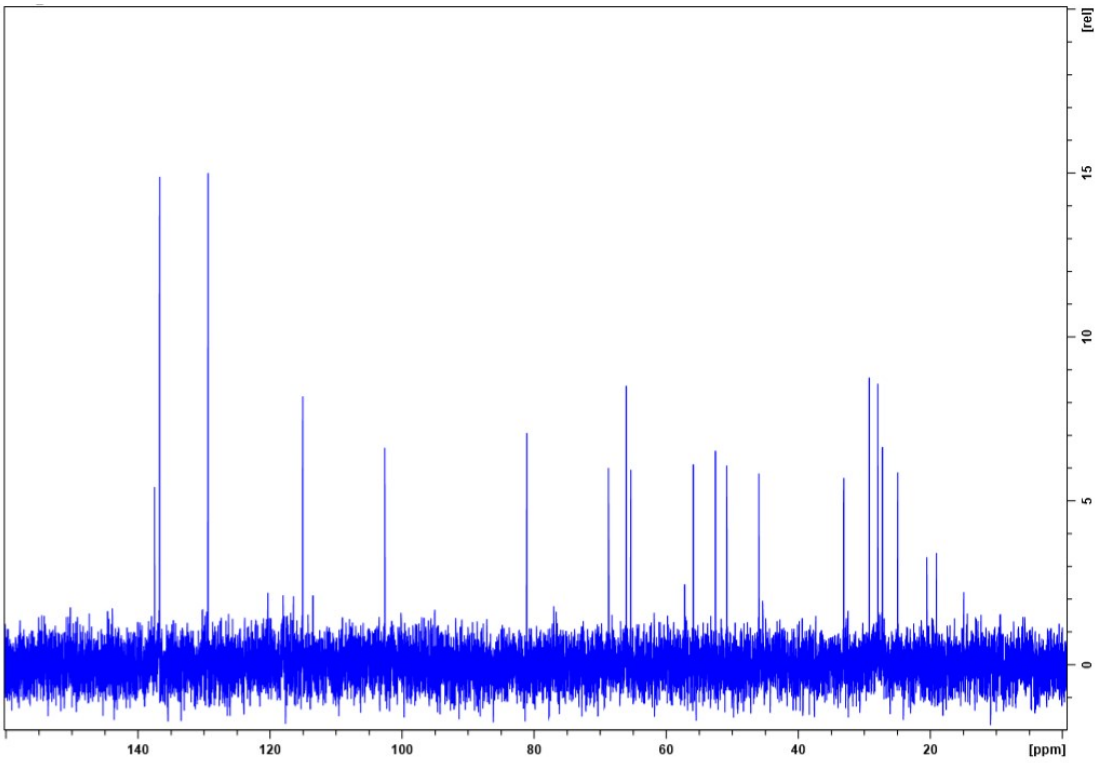

Fig. S46 ^{13}C spectrum (zoom) of PhB-Gly-Lys(*i*-Fru)-NH_2

Table S4 ^{13}C chemical shifts of the PhB in peptides.

Peptides	**^{13}C Chemical shifts [ppm]**
Fru1PhB2	132.47, 126.27
Fru1PhB3	132.17, 126.16
Fru1PhB4	126.1, 131.89, 133.99
Fru1PhB5	129.22 , 126.33, 133.96

5. ESI-MS spectra of hydrolysate

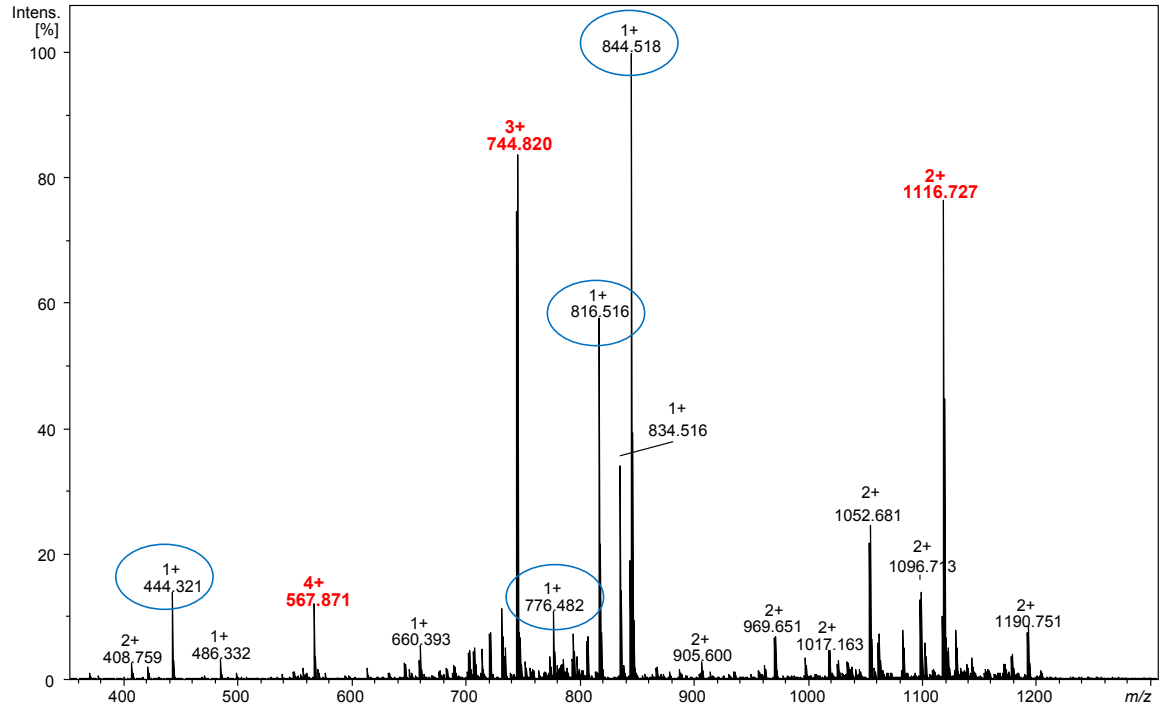

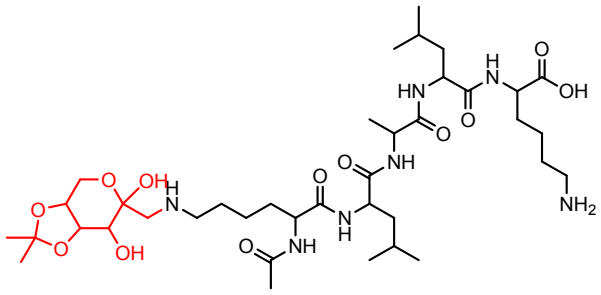

[M+H]$^+$ calc. 816.508

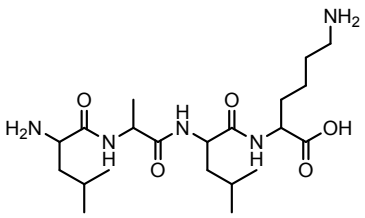

[M+H]$^+$ calc. 444.318

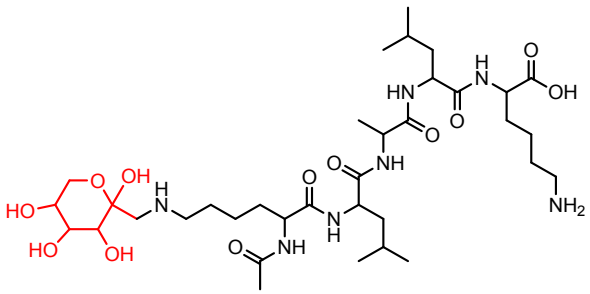

[M+H]$^+$ calc. 776.476

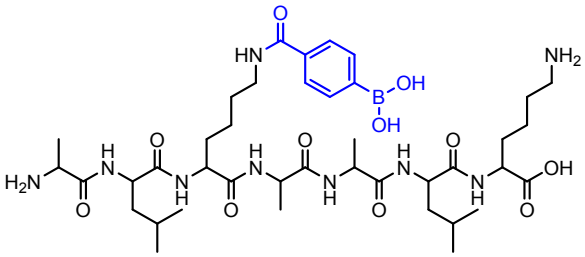

[M-H_2O+H]$^+$ calc. 844.497

Fig. S47 ESI-MS spectrum of tryptic hydrolysis products of Fru1PhB4 (below structure of identified products of hydrolysis with calculated *m/z*).

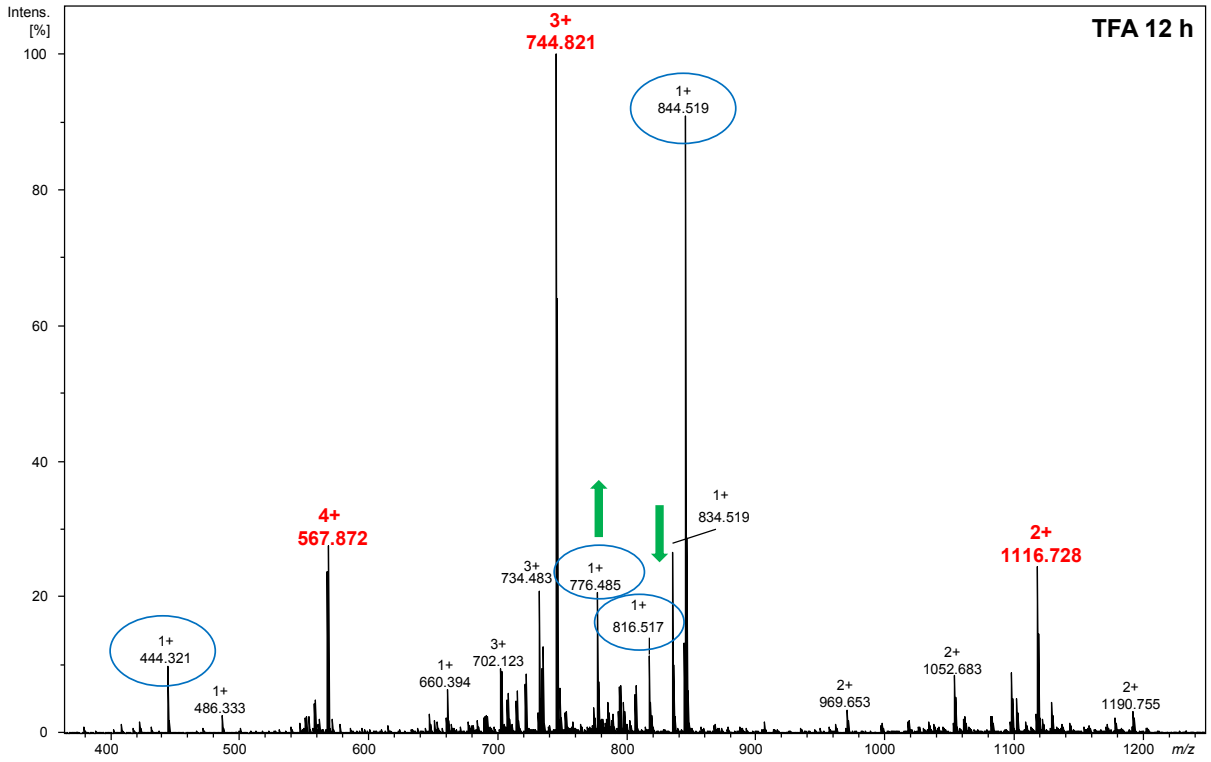

Fig. S48 ESI-MS spectrum of tryptic hydrolysis products of Fru1PhB4 after incubation in 95% solution of trifluoroacetic acid for 12h (green arrow – changing of signals intensity after incubation)

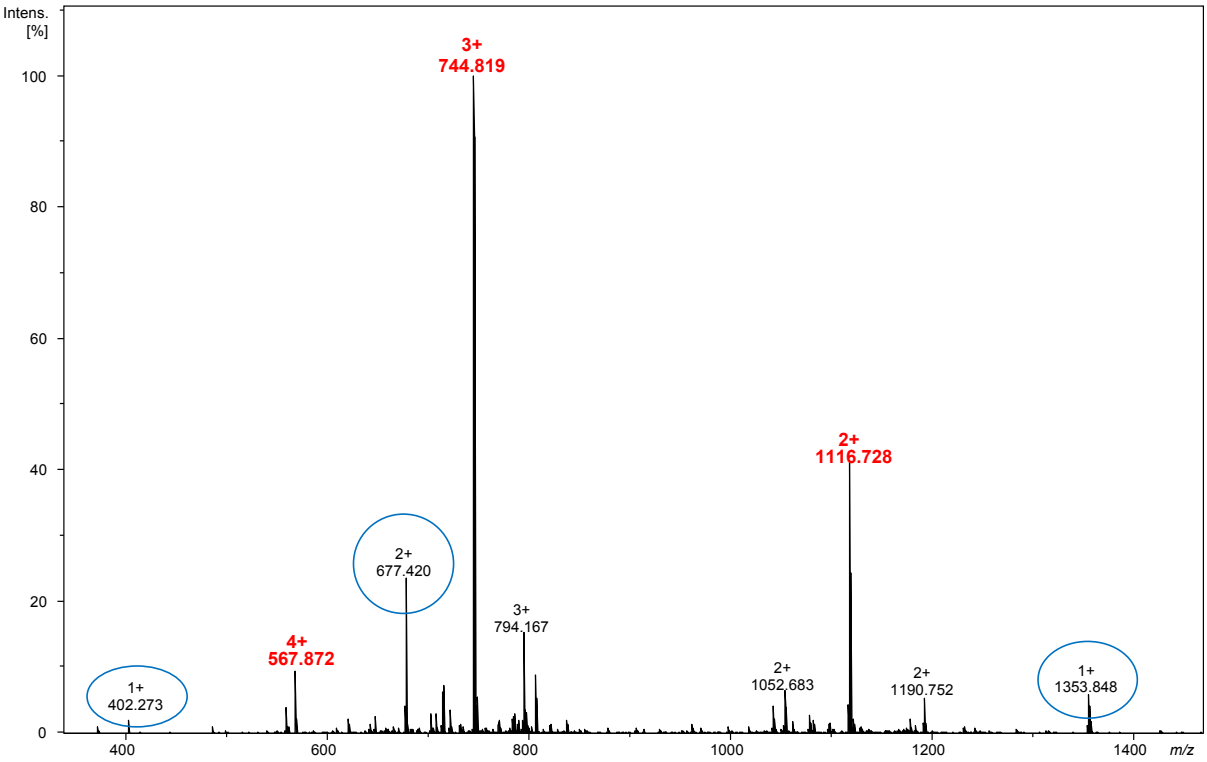

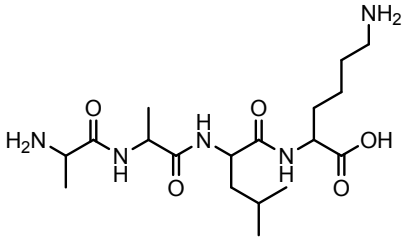

[M+H]$^+$ calc. 402.271

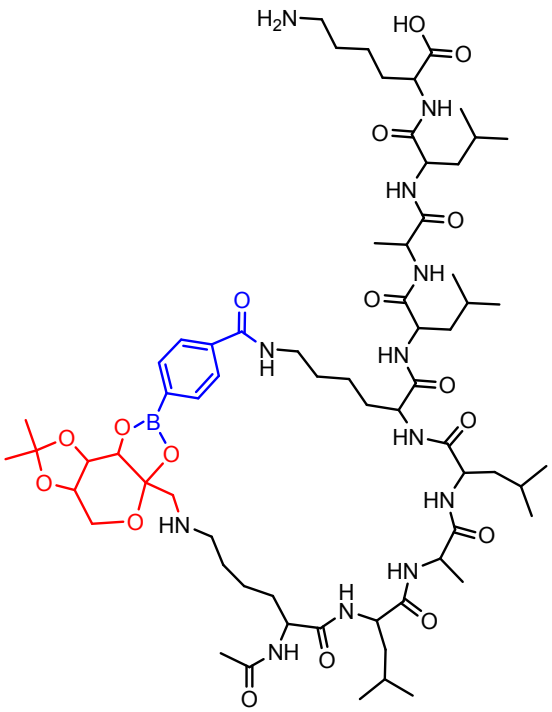

[M+H]$^+$ calc.1353.820

Fig. S49 ESI-MS spectrum of tryptic hydrolysis products of Fru1PhB2 (below structure of identified products of hydrolysis with calculated *m/z*).

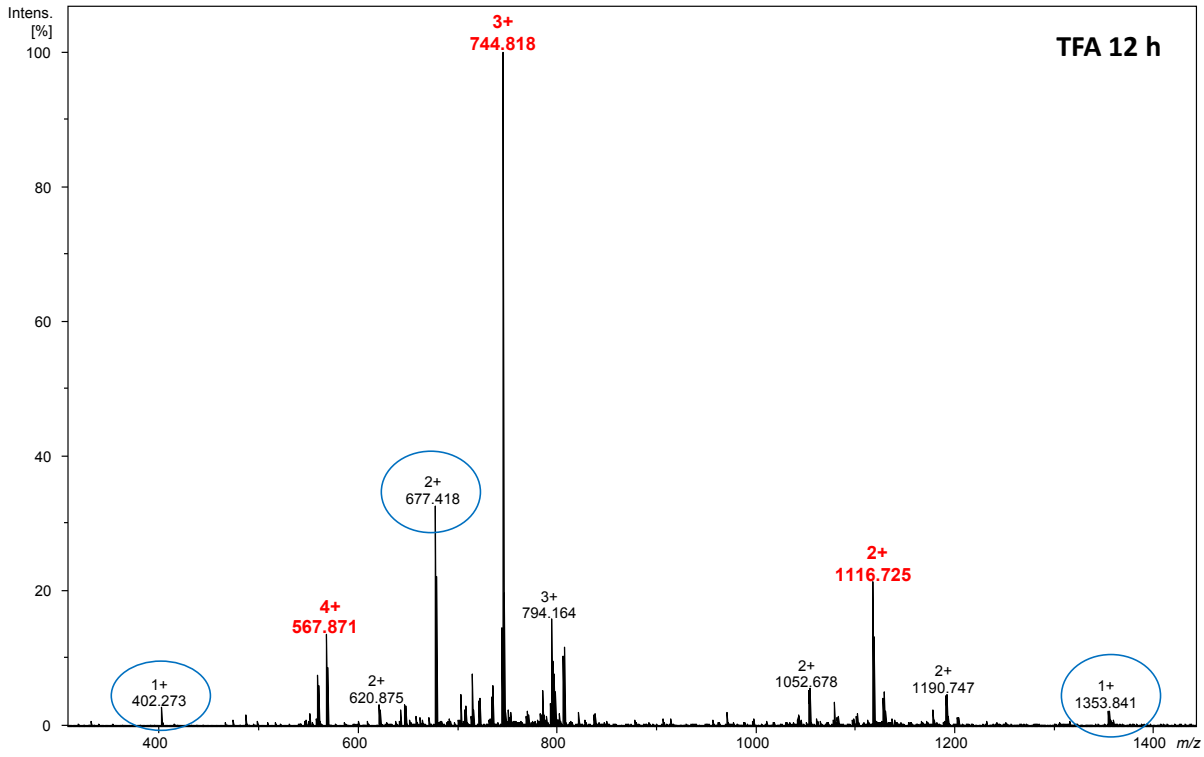

Fig. S50 ESI-MS spectrum of tryptic hydrolysis products of Fru1PhB2 after incubation in 90% solution of trifluoracetic acid for 12 h

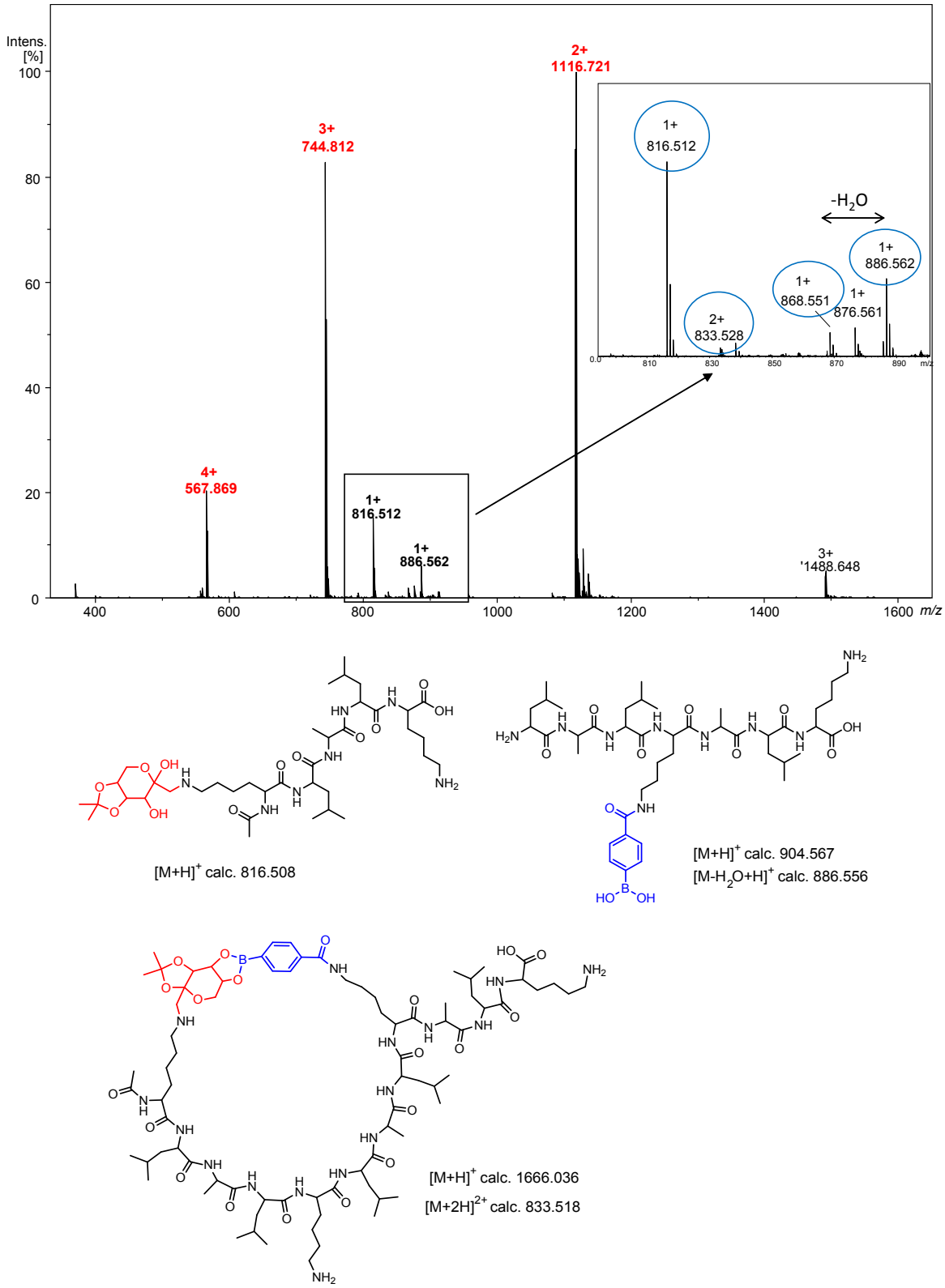

Fig. S51 ESI-MS spectrum of tryptic hydrolysis products of Fru1PhB3 (below structure of identified products of hydrolysis with calculated *m/z*).

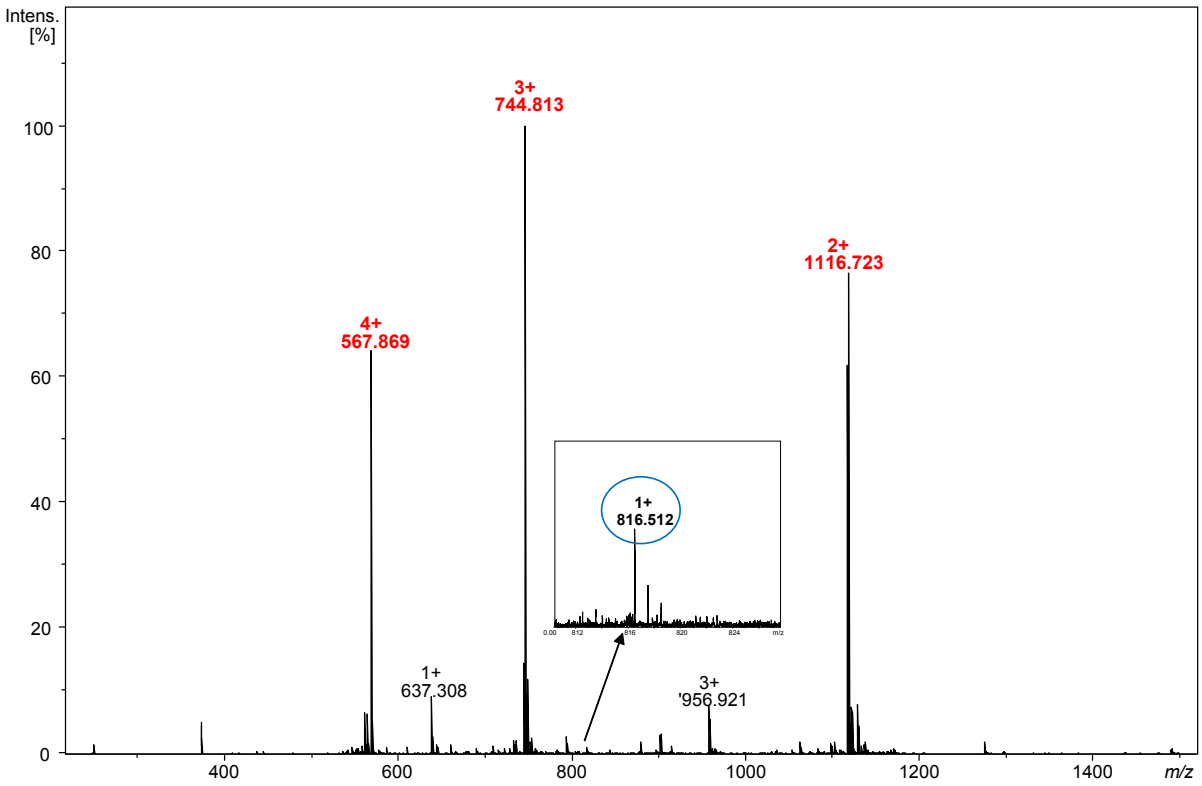

Fig. S52 ESI-MS spectrum of tryptic hydrolysis products of Fru1PhB5

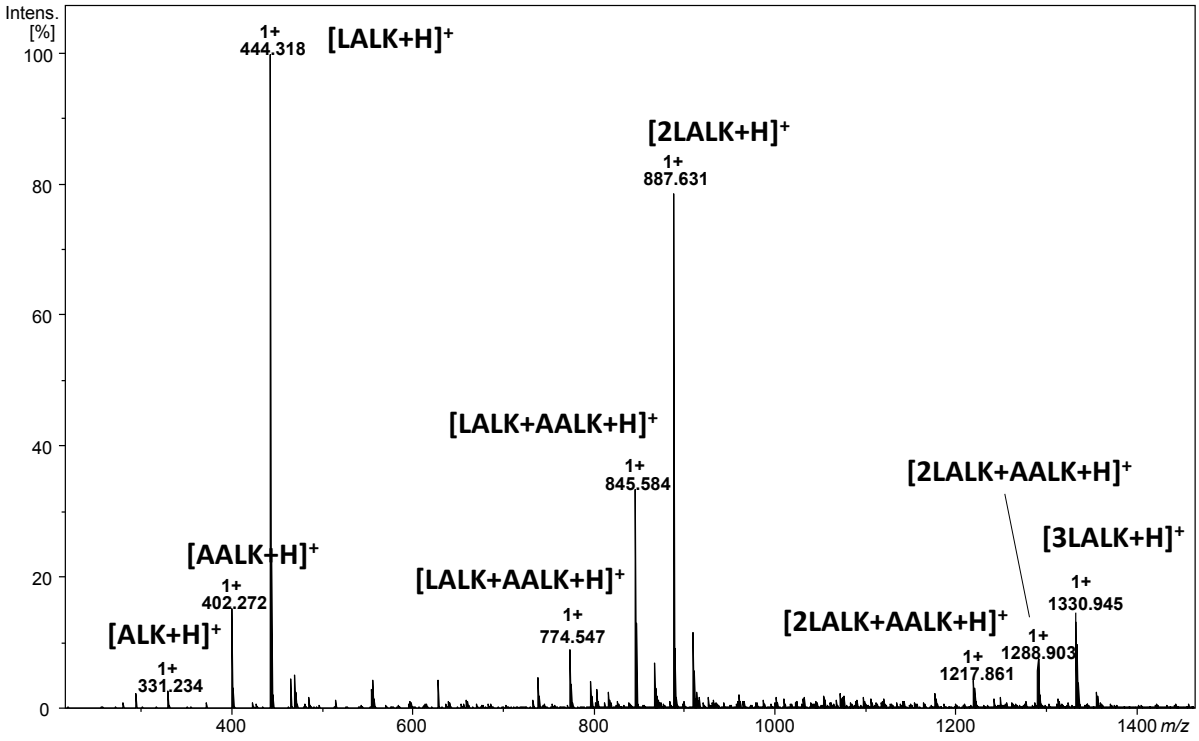

Fig. S53 ESI-MS spectrum of tryptic hydrolysis products of non-modified peptide Ac-MAP

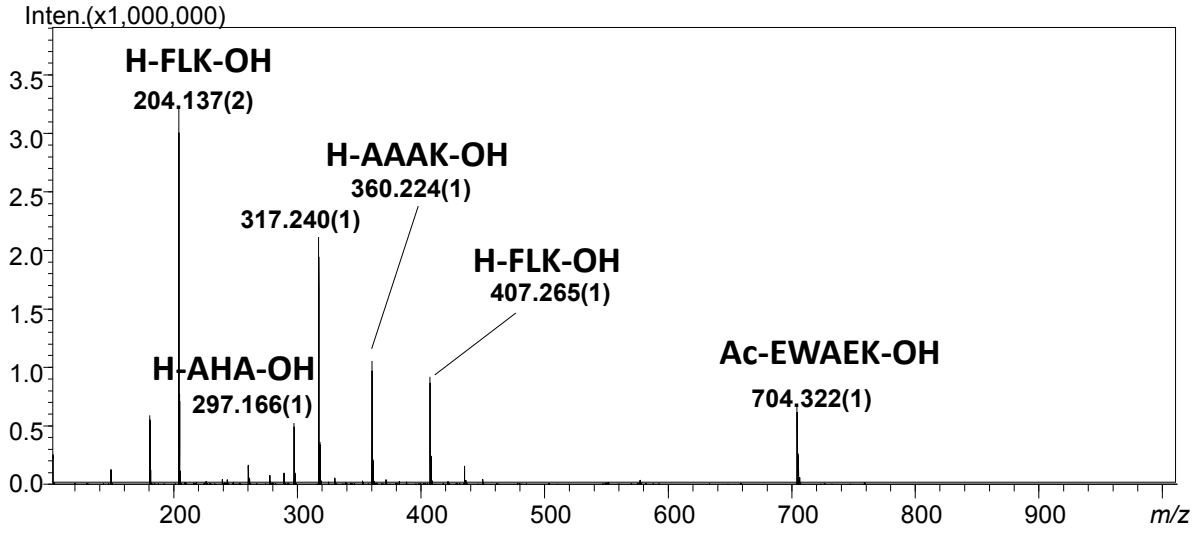

Fig. S54 ESI-MS spectrum of tryptic hydrolysis products of Ac-RNaseA*

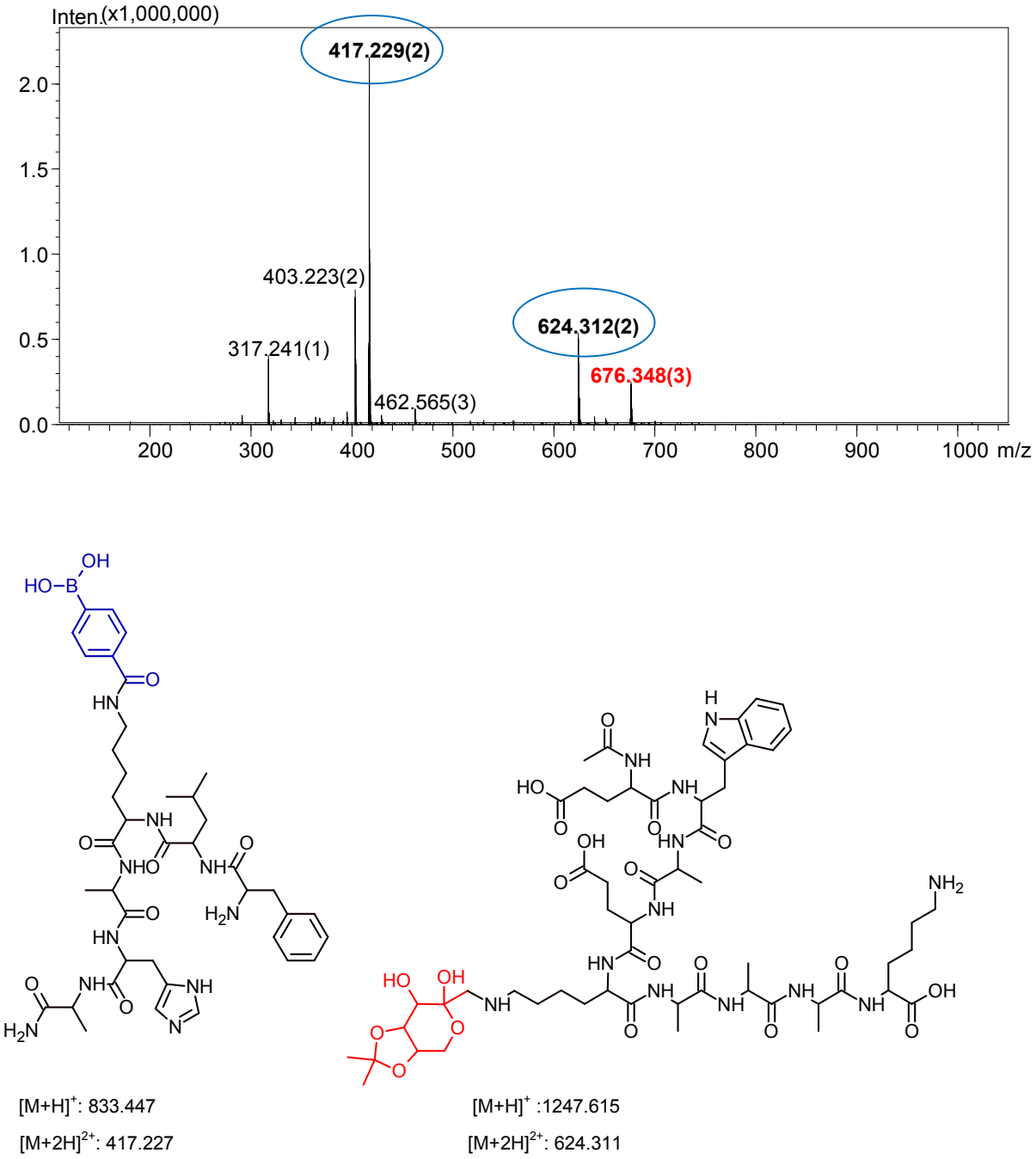

Fig. S55 ESI-MS spectrum of tryptic hydrolysis products of non-modified peptide Fru1PhB3*

6. Theoretical calculations using Avogadro: An Advanced Molecule Editor and Visualizer

Based on simple modeling, ideal geometry and van der Waals radii for atoms using an appropriate database ([1]- Avogadro: An Advanced Molecule Editor and Visualizer. https://avogadro.cc/ (2018) theoretical calculations concerning the forming of secondary

structure in stapled peptides (MAP analogues) were carried out. Below the experimental part and obtained results. This part was also placed in SI.

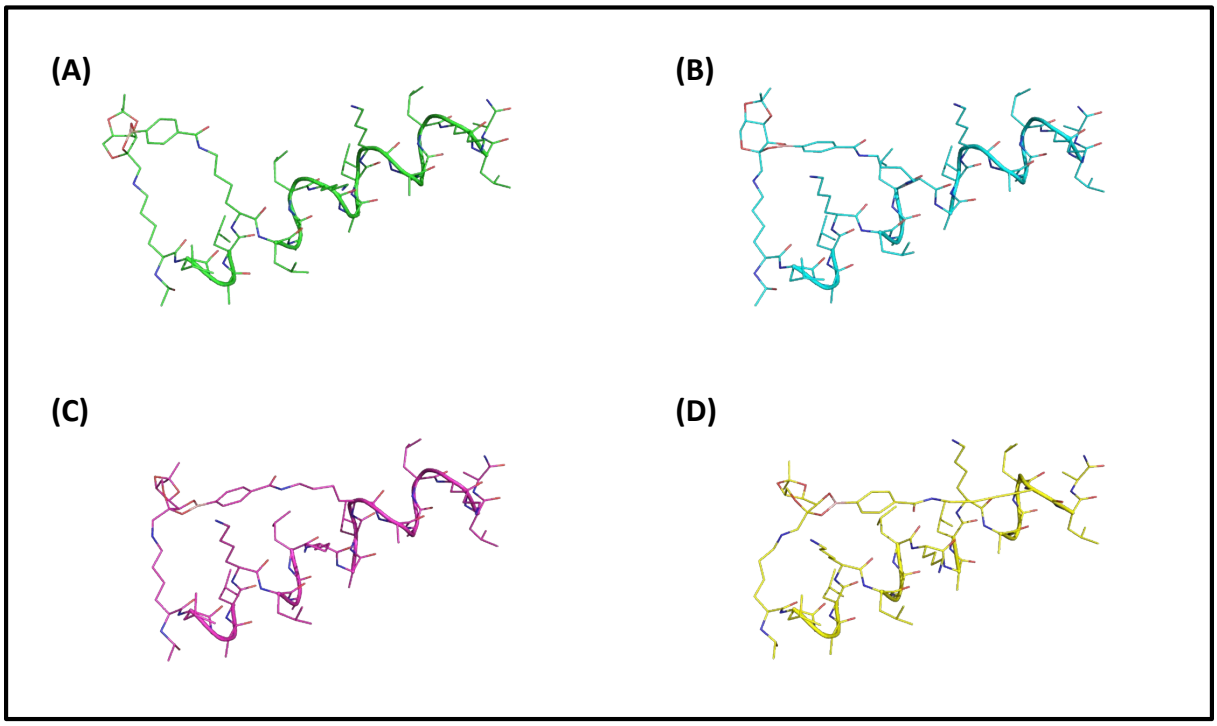

Fig. S56 Molecular modeling of (A) Fru1PhB2, (B) Fru1PhB3, (C) Fru1PhB4, and (D) Fru1PhB5.

The peptides were generated with Avogadro software [1] using peptide builder function. The structure was set as an alpha helix, L-stereochemistry, and the Torsion Angles were set to -60.00°and - 40.00° for phi and psi, respectively. The ends of the peptides were modified with N-terminal acetylation and C-terminal amidation. Phenylboronic acid and sugar residues were generated through draw tool and connected to Lysins accordingly. The peptides were subjected to geometry and molecular mechanics optimization with Avogadro software using Auto optimization tool. Universal field force (UFF) and the steepest descent algorithm were chosen as default settings for this optimization. The optimized molecular structures of the peptides were visualized and prepared for publication with Pymol software.

The molecular modeling of the peptides is presented in Fig 6. The structural geometry was optimized after the sugar residue on lysine 1 was connected to phenylboronic acid that is located on lysine 2 (Fig. 6A), lysine 3 (Fig. 6B), lysine 4 (Fig. 6C), and lysine 5 (Fig. 6D). The resulted structures indicate that the Fru1PhB4 peptide adopts a more stable helical conformation as compared to other peptides, which is supported by the CD (SI). The Fru1PhB2 peptide forms a shorter helix due to limited distance between the two moieties, whereas Fru1PhB3 and Fru1PhB5 show steric clashes that limit the helix stability.